PERTURBATIONS ON HYPERSONIC WEDGE FLOW

Thesis by

Norman David Malmuth

In Partial Fulfillment of the Requirements

For the Degree of

Doctor of Philosophy

California Institute of Technology

Pasadena, California

1962

ACKNOWLEDGEMENTS

The author expresses his appreciation for the invaluable assistance he received through numerous discussions with the director of this research, Professor Julian D. Cole of the California Institute of Technology. Also special thanks is given to Dr. Arthur Messiter for his helpful criticisms. Much inspiration and motivation was obtained through special courses in applied mathematics given by Professor Paco Lagerstrom of the Institute.

In addition, the author wishes to thank the following personnel of North American Aviation Inc. for the splendid cooperation in making a portion of the company facilities and time available for this work: Mr. Bill Martin, Chief, Preliminary Analysis Section, Mr. Bill Vance, Supervisor, Preliminary Analysis Section, Mr. Jack Bonner and Dr. Hans Mueller, Group Engineers, Flight Sciences Section, Mr. Fred Hall, Senior Engineer and Mr. Hugh Falcon of CEIR whose talent with respect to the IBM 7090 digital computor was of great assistance in the calculations.

Finally, a large debt of gratitude is owed to Mrs. Alrae Tingley for her painstaking efforts with respect to the manuscript, and Mrs. Electra Christensen for her help with the figures.

ABSTRACT

The hypersonic inviscid flow over a configuration representing a small perturbation about a two-dimensional wedge is analyzed. Equations and boundary conditions are obtained for a class of general perturbations within the framework of Hypersonic Small Disturbance Theory. A specialization of this formulation is made to the case where the resultant perturbation consists of two semi-infinite flat plates of slightly different incidence to the freestream. The flow over such a shape is divided into an outlying uniform region and a central conefield. Here, the outlying, uniform region solution is found to be trivial. The determination of the conefield gives rise to an elliptic boundary value problem which is solved with the aid of the Tschaplygin transformation and other conformal mappings.

Calculations are presented using the Fourier series solution for the perturbation pressure indicating the surface loads associated with the perturbation as well as the shock distortion function. Integral representations are obtained for the downwash and sidewash perturbations using the pressure solution.

The results are compared qualitatively with an analogous linear supersonic flow.

Finally, a solution for more general profiles is obtained under the further restriction that the specific heat ratio γ is close to one. This solution is specialized to the case considered previously and a qualitative evaluation of the physical significance of the results is made.

TABLE OF CONTENTS

I. INTRODUCTION

An interesting class of gasdynamic problems has recently been investigated that show promise of giving insight into the field structure of hypersonic flows. Moreover, the study of these questions could lead to the acquisition of techniques for the analysis of high Mach number interference phenomena, control surface aerodynamics and in a more general sense, wing camber and twist effects.

The fundamental idea employed in the formulation of these situations is the construction of a hypersonic flow that can be interpreted as a small perturbation about another known flow, henceforth referred to as the "basic flow." Such a perturbation may be achieved by making appropriate distortions to the body over which the basic flow takes place. For a suitable class of basic flows, and for a sufficiently small perturbation, it may be expected that a mathematically linear situation could arise. Hopefully, and in sharp contrast to the typical hypersonic small disturbance problem, the boundary conditions could be satisfied on the undistorted surfaces and the equations of motion would be of linear character. Since the wedge and cone have relatively simple fields, they are ideal basic shape choices. In particular, the uniform flow downstream of the wedge bow shock provides the least complicated environment for the assessment of the effect of perturbations.

Thus, if the wedge angle, δ, is vanishingly small, i.e. $O(1/M_\infty)$ as $M_\infty \to \infty$, where M_∞ is the freestream Mach number, and furthermore, if ϵ is another small quantity tending to zero independent of δ,

a thickness perturbation of $O(\delta\epsilon)$ produces a disturbance field with respect to the gas lying between the shock and body characterized by an effective supersonic-hypersonic similarity parameter, $H = \delta\epsilon M_1$. Here M_1 is the Mach number behind the bow shock of the undisturbed wedge flow and as such, can be thought of as an ambient quantity for the local conditions about the "bump." More precisely, if the requirements of Hypersonic Small Disturbance Theory* are assumed valid for the configuration at hand, M_1 will be much greater than one. In fact if:

$$H \equiv \frac{1}{M_\infty^2 \delta^2} \quad \text{fixed as} \quad \delta \to 0$$

then:

$$M_1 = \left[\frac{2}{\gamma(\gamma-1)}\right]^{1/2} \frac{1}{\delta} + O(\delta) \quad \text{as} \quad H \to 0$$

where γ is the specific heat ratio of the flow. Accordingly, outside of the cavity bounded by the secondary wave system emanating from the bump, the field is hypersonic, uniform and two-dimensional. However, a necessary condition for the existence of linear supersonic perturbations is that:

$$H_1 \ll 1$$

For the case at hand, it is obvious that this is the case providing γ is not too close to unity. Specifically:

$$H_1 = O(\epsilon) \quad \text{as} \quad \delta \to 0$$

Despite the fact that the previous condition is satisfied, a significant difference between the hypersonic and linear fields can be anticipated.

*Ref. 1, Chapter II provides a discussion of Hypersonic Small Disturbance Theory.

In the linear case, the bow shock or Mach wave which establishes the entropy and consequently the vorticity distribution downstream is the locus of Mach cones whose apices are located on the leading edge of the wedge. The semi-vertex angle of each cone is equal to $\sin^{-1}1/M_\infty$, so that for the case at hand, the Mach wave is a plane and makes a constant dihedral angle with the wedge surface along its span. The entropy jump across this Mach wave or weak shock is of the order of the cube of the characteristic flow deviation experienced in traversing it. Accordingly, the entropy gradient normal to the stream lines is of the same order, and hence, so is the vorticity. Moreover, since the velocity, density and pressure perturbations are of the first order in the deflection, the field of these variables is to all intents and purposes irrotational.

By contrast, the hypersonic case is characterized by strong shocks in the basic flow. As will be seen subsequently, the distortion of these shocks will introduce entropy and vortical perturbations of the first order in the flow deflection, invalidating the simplifications inherent in the irrotationality of the linear field. Furthermore, the topological structure of the boundaries will change due to the strength of the shock of the basic field, i. e., the strong hypersonic shock will no longer be the envelope of the Mach cones. As will be shown presently, the distortions of the shock wave will be negligible in terms of fixing the location of the shock boundary for the hypersonic perturbation problem. However, what is crucial in this case is the fact that individual fluid particles carry different entropy levels with them as they

travel downstream from the shock. One mathematical implication of the foregoing is that the initial or boundary values of the dependent variables are no longer piecewise constants as in the linear case, but continually varying quantities.

Guiraud, in a previous study (2), has analyzed thin wedges having two-dimensional distortions within the framework of Hypersonic Small Disturbance Theory (abbreviated HSD in what follows). Holt and Yim, in (3a) and (3b), consider two special three-dimensional distortions on thick wedges for arbitrary supersonic Mach numbers. Here, the perturbations are about the exact wedge field rather than the approximate HSD environment as in (2). Nevertheless, since H is in effect $O(1)$ in this case, the associated mathematical problem, except for some complication in the constants appearing in the boundary conditions is qualitatively of the same form as that which would have been obtained from a three-dimensional perturbation about an analogous HSD wedge field.

A major portion of the present research (given in Part II) will be concerned with the structure of the cone fields which were considered only superficially in the analysis of Holt and Yim. For this purpose, the HSD flow over the arrangement shown in figure 1 will be investigated. In the figure, an infinite span wedge is depicted, having its port and starboard sections rotated in opposite directions about the leading edge of the arrangement. The angle of rotation is such that the resulting "differential flap" configuration represents only a slight perturbation from the basic wedge profile. Here, a Mach cone having its axis of symmetry coincident with the x axis and its semi-apex

angle approximately equal to $1/M_1$ divides the flow downstream of the bow shock into a central cone field, and two outlying constant state regions. The central conical region has a structure qualitatively similar to those occurring in (3a). Such a configuration will have fundamental aspects, since more interesting flows can be obtained from it by superposition techniques such as Duhamel's integral. This property follows as a result of the stipulated linearity of the problem, and is directly analogous to the conical supersonic flows discussed in (4) and (5).

However, as indicated previously, significant differences do exist between the HSD and linear supersonic regimes. These will be made clearer in part II from a consideration of a configuration analogous to that of figure 1 within the framework of linearized supersonic theory.

In the final portion of this work, contained in part III, a generalization of the existing results to more arbitrary three-dimensional perturbations is given. Here, the body distortions are of $O(\delta\epsilon)$ in the HSD limit and the further restriction is made over and above those of HSD theory that $\frac{\epsilon}{\gamma-1} \to 0$ as $\gamma \to 1$. The solution of the mathematical problem obtained under this simplifying assumption is called a Newtonian approximation, and gives all the flow properties in terms of the arbitrary body distortion function. From these results, a specialization is made to the geometry considered in part II, and the qualitative effects of the Newtonian approximation on the previous cone field structure is discussed briefly.

To complete part III, the mathematical problem leading to a "strip theory" for arbitrary distortional profiles is solved. Here, adjacent lateral stations do not interact, and the role of the application in previous sections of certain coordinate distortions is vividly illustrated.

II. THE FLOW OVER A PAIR OF DIFFERENTIALLY DEFLECTED PANELS ACCORDING TO HYPERSONIC SMALL DISTURBANCE THEORY

1. Basic Equations

With the axis convention indicated in figure 1, the flow over the surface given by:

$$B(\bar{x}, \bar{y}, \bar{z}) = \bar{y} - \delta[\bar{x} + \epsilon f(\bar{x}, \frac{\bar{z}}{b})] = 0 \qquad (1)$$

will be studied. Ultimately, these considerations will be specialized to the case where $f = \operatorname{sgn} z$. However, at the outset, to preserve generality, it will be profitable to consider the arbitrary perturbation. Moreover, the mathematical formulations of both problems differ only slightly. δ in equation 1 is the basic wedge angle, ϵ measures the deviation from the basic shape, and finally, b is a characteristic lateral length to be related to the Mach cone apex angle discussed previously. b may be thought of as a wave length depending on the nature of the lateral perturbative fluctuations for its mode of definition. The definition of b will be amplified upon presently.

Within this framework, the following limit will be considered:

$$\text{(a)} \quad H = \frac{1}{M_\infty^2 \delta^2} \text{ fixed as } \delta, \epsilon \to 0 \text{ independently} \qquad (2)$$

$$\text{(b)} \quad H \to 0$$

M_∞ in equation 2 is the Mach number of the freestream and H is the hypersonic similarity parameter for this problem.

As a working hypothesis, the shock will be postulated to have the following representation:

$$S(\bar{x}, \bar{y}, \bar{z}) = \bar{y} - \delta[\theta\bar{x} + \epsilon g(\bar{x}, \frac{\bar{z}}{b})] = 0 \qquad (3)$$

Clearly, the first member in the brackets of equation 3 represents the shock elevation for no wedge distortion. Hence, the second is the effect resulting from the perturbation. If $\vec{q}$, ρ, P and γ respectively represent the velocity, density, pressure and specific heat ratio of the gas flowing over the obstacle, then the exact equations governing the inviscid motion of the medium are:

$$\nabla \cdot \rho\vec{q} = 0 \qquad \text{continuity} \qquad (4a)$$

$$\vec{q} \cdot \nabla\vec{q} = -\frac{\nabla P}{\rho} \qquad \text{momentum} \qquad (4b)$$

$$\vec{q} \cdot \nabla \frac{P}{\rho^{\gamma}} = 0 \qquad \text{entropy} \qquad (4c)$$

The class of flows for which:

$$b = \frac{\delta}{\Lambda} \quad \text{where } \Lambda \text{ is fixed as } \delta \to 0 \qquad (5)$$

will now be considered. If $P(\bar{x}, \bar{y}, \bar{z})$ is a point in the region of interest, (between shock and body and $\bar{z} = O(b)$) as $\delta \to 0$, then

$$\bar{x} = O(1)$$

$$\bar{y} = O(\delta) \qquad \text{as } \delta \to 0$$

$$\bar{z} = O(\delta)$$

Accordingly, the following coordinate system is selected to keep the relative position of P with respect to the physical boundaries of the problem invariant for all δ as $\delta \to 0$.

$$x = \bar{x}, \quad y = \bar{y}/\delta, \quad z = \bar{z}/\delta \tag{6}$$

For the limiting process described, the following asymptotic expansion for $\vec{q}$ is assumed:

$$\frac{\vec{q}(\bar{x}, \bar{y}, \bar{z}; M_\infty, \delta, b, \epsilon)}{U} = \vec{i}\,[1 + \delta^2(u_o + \epsilon u) + O(\delta^4, \epsilon^2\delta^2)$$
$$+ \vec{j}\,[\delta(v_o + \epsilon v) + O(\delta^3, \epsilon^2\delta)]$$
$$+ \vec{k}\,[\delta\epsilon\, w(x, y, z; H, \Lambda) + O(\delta^3, \epsilon^2\delta)] \tag{7a}$$

Furthermore, the pressure and density representations are:

$$\frac{P - P_\infty}{\rho_\infty U^2} = \delta^2 p_o[1 + \epsilon p] + O(\delta^4, \delta^2\epsilon^2) \tag{7b}$$

$$\frac{\rho}{\rho_\infty} = \sigma_o[1 + \epsilon\sigma] + O(\delta^2, \epsilon^2) \tag{7c}$$

Noting that:

$$\nabla \equiv \left[\frac{\partial}{\partial \bar{x}}, \frac{\partial}{\partial \bar{y}}, \frac{\partial}{\partial \bar{z}}\right] = \left[\frac{\partial}{\partial x}, \frac{1}{\delta}\frac{\partial}{\partial y}, \frac{1}{\delta}\frac{\partial}{\partial z}\right] \tag{8}$$

and

$$\vec{q} \cdot \nabla = U\left[\frac{\partial}{\partial x} + (v_o + \epsilon v)\frac{\partial}{\partial y} + \epsilon w \frac{\partial}{\partial z} + O(\epsilon^2, \delta^2)\right] \tag{9}$$

the substitution of the expansions 7 and equations 8 and 9 into equation 4a gives the succeeding approximate equations when terms of the indicated orders are retained:

$O(1)$:

$$\frac{\partial \sigma_o}{\partial x} + \frac{\partial(\sigma_o v_o)}{\partial y} = 0 \tag{10a}$$

$O(\epsilon)$:

$$\frac{\partial \sigma}{\partial x} + \frac{\partial v}{\partial y} + v_o \frac{\partial \sigma}{\partial y} + \frac{\partial w}{\partial z} = 0 \tag{10b}$$

Again, in a similar manner, equation 4b gives the ensuing approximate relations:

x-Momentum

$O(\delta^2)$:

$$\left(\frac{\partial}{\partial x} + v_o \frac{\partial}{\partial y} \right) u_o = - \frac{1}{\sigma_o} \frac{\partial p_o}{\partial x} \tag{11a}$$

$O(\delta^2 \epsilon)$:

$$\left(\frac{\partial}{\partial x} + v_o \frac{\partial}{\partial y} \right) u = - \frac{p_o}{\sigma_o} \frac{\partial p}{\partial x} \tag{11b}$$

y-Momentum

$O(\delta)$:

$$\left(\frac{\partial}{\partial x} + v_o \frac{\partial}{\partial y} \right) v_o = - \frac{1}{\sigma_o} \frac{\partial p_o}{\partial y} \tag{12a}$$

$O(\delta \epsilon)$:

$$\left(\frac{\partial}{\partial x} + v_o \frac{\partial}{\partial y} \right) v = - \frac{p_o}{\sigma_o} \frac{\partial p}{\partial y} \tag{12b}$$

z-Momentum

$O(\delta \epsilon)$:

$$\left(\frac{\partial}{\partial x} + v_o \frac{\partial}{\partial y} \right) w = - \frac{p_o}{\sigma_o} \frac{\partial p}{\partial z} \tag{13}$$

Finally, application of the substitution procedure to equation 4c gives:

$O(1)$:

$$\left(\frac{\partial}{\partial x} + v_o \frac{\partial}{\partial y} \right) \frac{p_o}{\sigma_o^\gamma} = 0 \tag{14a}$$

$O(\epsilon)$:

$$\left(\frac{\partial}{\partial x} + v_o \frac{\partial}{\partial y}\right)(p - \gamma\sigma) = 0 \tag{14b}$$

Since the quantities with subscript o, (zeroth order) play the role of the basic flow properties, they have been treated as constants in the formulation for the quantities with subscript 1 (first order).

2. Boundary Conditions

To complete the derivation of the approximate problem, it will be necessary to determine a set of boundary conditions for the asymptotic representations of the dependent variables. In this connection, the principle boundaries to be considered are the shock and body surfaces. In the case of certain classes of obstacles whose surfaces are ruled from a point, an additional boundary, namely a Mach cone emanating from the point is to be considered, in order for the problem to be properly posed in a mathematical sense.

For the case at hand, the shock is assumed to possess the functional continuity properties which allow each infinitesimally small surface element comprising it to be considered independently of the others. Furthermore, since the gas is considered inviscid, there exist no shear forces to change the tangential component of the flow as it crosses shock. In other words, the perturbation component of the velocity immediately behind the wave is normal to it. Formally, this can be expressed as:

$$(\vec{q} - U\vec{i}) \times \nabla S = 0 \tag{15}$$

Substitution of equations 7a and 3 into equation 15 yields the following relationship between terms of $O(\delta\epsilon)$:

$$w_s \equiv w(x, \theta x + \epsilon g, z) = - v_o \Lambda g_{(2)} \quad * \tag{16a}$$

If it is assumed that the function w has the required properties, then it can be developed into the following Taylor's series about the point $(x, \theta x, z)$:

$$w_s = w(x, \theta x, z) + \epsilon g w_y(x, \theta x, z) + O(\epsilon^2)$$

Hence, the boundary condition involving w becomes in the limit as $\epsilon \to 0$:

$$w(x, \theta x, z) = - v_o \Lambda g_{(2)} \tag{16b}$$

The determination of the interrelations between the other shock quantites, can be facilitated by a consideration of the pseudo-one-dimensional gas motion that exists behind a small surface element of the shock wave. Accordingly, if a Galilean transformation is performed so as to move the point of observation downstream in the flow with a velocity $U\vec{i}$, the gas ahead of the shock will have zero velocity in the new coordinates. Behind the shock, it will have the velocity $\vec{q} - U\vec{i}$. Since this vector is normal to the shock, it can be thought of as having been produced by a piston whose face is parallel to the shock surface element. Since the piston is not porous, the magnitude of its velocity, u_p is the same as the resultant gas velocity. Thus,

---

* $g_{(2)}$ denotes the derivative of g with respect to its second argument.

$$u_F = \left| \vec{q} - U \vec{i} \right| \tag{17}$$

In this model then, the equivalent wave speed, c, i. e., the speed of the wave as it moves into the undisturbed gas normal to itself is:

$$c = U \vec{i} \cdot \frac{\nabla S}{|\nabla S|} \tag{18}$$

The consideration of the physical conservation laws applied to a cylinder of gas as the shock passes over it yields the following relations for the pressure P_F, density ρ_F, and velocity u_F of the piston in terms of the ambient quantities P_I and ρ_I,

$$c^2 - \frac{\gamma+1}{2} c u_F - a_I^2 = 0 \tag{19a}$$

$$P_F - P_I = \rho_I c u_F \tag{19b}$$

$$\rho_F (c - u_F) = \rho_I c \tag{19c}$$

Application of equation 19 to the case at hand can be effected by substitution for u_F and c from equations 17 and 18. Recognizing that $M_\infty = \infty$ can be obtained by letting $a_I = 0$, we find:

$$c = \frac{\gamma+1}{2} \left[U \delta v_{o_s} \left(1 + \frac{\epsilon v_s}{v_{o_s}}\right)\right] \tag{20}$$

Equating terms of the same order of magnitude using the expression for c, i. e., equation 18 in 20:

$$v_{o_s} = \frac{2}{\gamma+1} \theta \tag{21a}$$

$$v_s = \frac{2}{\gamma+1} g_x \tag{21b}$$

Also:

$$\frac{P_F - P_I}{\rho_I U^2} = \frac{\gamma+1}{2} \delta^2 [1 + 2\epsilon v_s] v_{o_s}^2$$

Thus:

$$p_{o_s} = \frac{\gamma+1}{2} v_{o_s}^2 \tag{22a}$$

$$p_s = (\gamma+1) \frac{v_{o_s}^2}{p_{o_s}} v_s \tag{22b}$$

Finally, since:

$$\frac{\rho_I}{\rho_F} = \frac{\rho_\infty}{\rho_s} = 1 - \frac{u_F}{c} = 1 - \frac{2}{\gamma+1} = \frac{\gamma-1}{\gamma+1}$$

we find that:

$$\frac{\rho_s}{\rho_\infty} = \sigma_{o_s}(1 + \epsilon\sigma_s) + O(\delta^2, \epsilon^2)$$

which implies:

$$\sigma_{o_s} = \frac{\gamma+1}{\gamma-1} \tag{23a}$$

$$\sigma_s = 0 \tag{23b}$$

At the body, the kinematic condition that the normal velocity component of the gas is identical to that of the body can be expressed as:

$$\vec{q} \cdot \nabla B = 0 \tag{24}$$

This reduces to:

$$v_{o_B} = v_o(x, x, z) = 1 \tag{25a}$$

$$v_B = v(x, x, z) = f_x(x, z) \tag{25b}$$

Throughout the derivation of the boundary conditions, it has been

assumed that the functions p, w, v, ρ are sufficiently well behaved to validate the application of the following representations in the neighborhood of the boundaries:

$$\Phi_B \equiv \Phi[x, x+\epsilon f, z] \doteq \Phi[x, x, z] + O(\epsilon) \text{ as } \epsilon \to 0 \qquad (26a)$$

$$\Phi_s \equiv \Phi[x, x+\epsilon g, z] \doteq \Phi[x, \theta x, z] + O(\epsilon) \text{ as } \epsilon \to 0 \qquad (26b)$$

where

$$\Phi = (\rho, v, w, p)$$

Summary of Equations and Boundary Conditions

Zeroth order:

$$\left.\begin{aligned} &\frac{\partial \sigma_o}{\partial x} + \frac{\partial \sigma_o v_o}{\partial y} = 0, && \text{continuity} \\ &Du_o = -\frac{1}{\sigma_o}\frac{\partial p_o}{\partial x}, && \text{x-momentum} \\ &Dv_o = -\frac{1}{\sigma_o}\frac{\partial p_o}{\partial y}, && \text{y-momentum} \\ &D\frac{p_o}{\sigma_o^\gamma} = 0, && \text{energy} \end{aligned}\right\}$$

$$D \equiv \frac{\partial}{\partial x} + v_o \frac{\partial}{\partial y}$$

$$p_{o_s} = \frac{\gamma+1}{2} v_{o_s}^2$$

$$v_{o_s} = v_o(x, \theta x, z) = \frac{2\theta}{\gamma+1}$$

$$\sigma_{o_s} = \frac{\gamma+1}{\gamma-1}$$

$$v_{o_B} = 1$$

First order:

$$\frac{\partial \sigma}{\partial x} + \frac{\partial v}{\partial y} + v_o \frac{\partial \sigma}{\partial y} + \frac{\partial w}{\partial z} = 0 \qquad \text{continuity}$$

$$Du + \frac{p_o}{\sigma_o} \frac{\partial p}{\partial x} = 0 \qquad \text{x-momentum}$$

$$Dv + \frac{p_o}{\sigma_o} \frac{\partial p}{\partial y} = 0 \qquad \text{y-momentum}$$

$$Dw + \frac{p_o}{\sigma_o} \frac{\partial p}{\partial z} = 0 \qquad \text{z-momentum}$$

$$D(p - \gamma\sigma) = 0 \qquad \text{energy}$$

$$w_s \equiv w(x, \theta x, z) = - v_o \Lambda g_{(2)}(\bar{x}, \frac{\bar{z}}{b})$$

$$v_s = \frac{2}{\gamma+1} g_x$$

$$p_s = \frac{(\gamma+1) v_{o_s}^2}{p_{o_s}} v_s$$

$$\sigma_s = 0$$

$$v_B \equiv v(x, x, z) = f_x(x, z)$$

3. Solution of the Zeroth Order Problem

The following constant state solution representing the HSD limit, ($H = 0$) of wedge flow, solves the zeroth order equations and boundary conditions uniquely:

$$v_o = 1 \qquad (27a)$$

$$p_o = \frac{\gamma+1}{2} \qquad (27b)$$

$$\sigma_o = \frac{\gamma+1}{\gamma-1} \tag{27c}$$

$$\theta = \frac{\gamma+1}{2} \tag{27d}$$

4. Solution of the First Order Problem

Because of the mode of appearance of the backwash, u in the equations and boundary conditions, it is possible to determine it after the hyperbolic system involving σ, v, w and p is solved. That is, it is possible to construct a properly posed initial value problem for the latter four quantities by ignoring the x-momentum equation completely. In the problem, the shock and body form time-like manifolds which bear the boundary data. Thus, the following system is to be considered using the information obtained from the zeroth order solution:

$$D\sigma + v_y + w_z = 0, \qquad \text{(continuity)} \tag{28a}$$

$$Dv + \frac{\gamma-1}{2} p_y = 0 \qquad \text{(vertical momentum)} \tag{28b}$$

$$Dw + \frac{\gamma-1}{2} p_z = 0 \qquad \text{(lateral momentum)} \tag{28c}$$

$$D(p - \gamma\sigma) = 0 \qquad \text{(entropy)} \tag{28d}$$

where

$$D \equiv \frac{\partial}{\partial x} + \frac{\partial}{\partial y} \tag{29}$$

Now, from the entropy equation:

$$\frac{Dp}{\gamma} = D\sigma \tag{30}$$

Substitution of the latter relation for $D\sigma$ into the continuity equation 28a gives:

$$\frac{Dp}{\gamma} + v_y + w_z = 0 \tag{31}$$

Using the zeroth order continuity equation, we may define the stream function of the undisturbed wedge flow as:

$$\psi_y = \sigma_o = \frac{\gamma+1}{\gamma-1}, \qquad \psi_x = -\sigma_o v_o = \frac{\gamma+1}{\gamma-1} \tag{32}$$

Now on the stream surfaces:

$$\psi(x, y) = \text{constant}$$

$$d\psi = 0 = \psi_x dx + \psi_y dy$$

or:

$$\frac{dy}{dx} = -\frac{\psi_x}{\psi_y} = \frac{\sigma_o v_o}{\sigma_o} = v_o = 1$$

Hence, the stream surfaces of the basic wedge flow are given by:

$$\psi = y - x = \text{constant} \tag{33}$$

A simplification is obtained by writing the system in the independent variables (x^*, ψ, z^*), where:

$$x^* = x, \quad \psi = y-x, \quad z^* = z \tag{34}$$

Accordingly, under the mapping:

$$(x, y, z) \rightarrow (x^*, \psi, z^*) \tag{35}$$

the differential operators transform as follows:

$$\frac{\partial}{\partial x} = \frac{\partial}{\partial x^*}\frac{\partial x^*}{\partial x} + \frac{\partial}{\partial \psi}\frac{\partial \psi}{\partial x} = \frac{\partial}{\partial x} - \frac{\partial}{\partial \psi} \tag{36a}$$

$$\frac{\partial}{\partial y} = \frac{\partial}{\partial \psi}\frac{\partial \psi}{\partial y} = \frac{\partial}{\partial \psi} \tag{36b}$$

$$\frac{\partial}{\partial z} = \frac{\partial}{\partial z^*} \tag{36c}$$

$$D = \frac{\partial}{\partial x^*} \tag{36d}$$

Also, we note that when:

$$y = y_s = \theta x = \frac{\gamma+1}{2}x$$

$$\psi = \psi_s = (\theta-1)x = \frac{\gamma-1}{2}x \tag{37}$$

Furthermore, when:

$$y = y_B = x$$

$$\psi = \psi_B = 0$$

so that, under the mapping,35, the equations and boundary conditions for a problem involving p, v and w as dependent variables are:

$$\left.\begin{aligned} &\frac{p_x}{\gamma} + v_\psi + w_z = 0 && (38a)\\ &v_x + \frac{\gamma-1}{2}p_\psi = 0 && (38b)\\ &w_x + \frac{\gamma-1}{2}p_z = 0 && (38c)\end{aligned}\right\}$$

$$v_B = v(x, 0, z) = f_x \tag{39a}$$

$$p_s = 2v_s = p(x, \frac{\gamma-1}{2}, x, z) = \frac{4}{\gamma+1}g_x \tag{39b}$$

$$w_s = -\Lambda g_z \tag{39c}$$

Here, the star notation has been dropped for brevity and Physicist's notation has been used, i. e. $v(x, y, z) = v(x, \psi, z)$.

4. 1. Specialization to the Differential Panel Configuration

Our considerations will now be concerned with the case for which:

$$b = \delta \longleftrightarrow A = 1 \tag{40a}$$

$$f = x \operatorname{sgn} z \tag{40b}$$

where:

$$\operatorname{sgn} z = 1 \qquad \text{for} \quad z > 0$$

$$\operatorname{sgn} z = -1 \qquad \text{for} \quad z < 0$$

An illustration of such a configuration is given in figure 1. Under these circumstances, the boundary conditions now become:

$$v_B = v(x, 0, z) = \operatorname{sgn} z \tag{41a}$$

$$p_s = 2v_s = \frac{4}{\gamma+1} g_x \tag{41b}$$

$$w_s = -g_z \tag{41c}$$

Obviously, the equations of motion are unaffected by this specialization. The equation satisfied by p can be obtained from the above system by elimination of the other dependent variables by cross differentiation. Thus, v may be eliminated from the first order system,

$$\left.\begin{aligned} \frac{p_x}{\gamma} + v_\psi + w_z &= 0 \\ \frac{\gamma-1}{2} p_\psi + v_x &= 0 \end{aligned}\right\}$$

by differentiating the top equation with respect to x and the bottom one with respect to ψ. Subtracting, one obtains:

$$\frac{p_{xx}}{\gamma} - \frac{\gamma-1}{2} p_{\psi\psi} + w_{zx} = 0$$

Differentiation with respect to z in equation 38c gives

$$w_{xz} = - \frac{(\gamma-1)}{2} p_{zz}$$

Substitution for w_{xz} in the above equation for p yields finally:

$$\frac{2}{\gamma(\gamma-1)} p_{xx} - p_{\psi\psi} - p_{zz} = 0 \quad * \qquad (42)$$

Thus, p obeys the wave equation. Here, the quantity $c^2 = \gamma(\gamma-1)/2$ can be shown to be the speed at which pressure waves caused by the bump travel in (ψ, z) planes. It is determined solely by the basic flow, like all other propagation characteristics of the disturbed flow including the capacity to convect mass, momentum and energy. From the discussion in the introduction it is apparent that:

$$\frac{\gamma(\gamma-1)}{2} = \frac{1}{M_1^2 \delta^2} = H_1 = c^2 \qquad (43)$$

4. 2. Determination of the Pressure-Conical Similarity

Returning to the system,38 we now note that the mapping:

$$(x, \psi, z) \rightarrow (\alpha x, \alpha\psi, \alpha z)$$

leaves the general form of the equations and boundary conditions invariant,

* This is the same equation for the pressure as obtained in ordinary linearized supersonic theory.

providing that the shock and body distortion functions, f and g are assumed homogeneous of order one. A sufficient condition for the foregoing invariance property to be exhibited is that the dependent variables themselves are zeroth order homogeneous. This conical symmetry allows the dependent variables to be written in the following form:

$$\Phi = \Phi(\Psi, Z) \tag{44}$$

where

$$\Phi = p, v, w$$

and

$$\Psi = \frac{\psi}{cx}, \quad Z = \frac{z}{cx} \tag{45}$$

In accord with the restriction indicated previously:

$$g = xG(Z) \tag{46}$$

where the coordinates have been normalized for convenience. With this conical dependence, the panel problem will now be reformulated. In accord with this, new representations for the boundaries will be found in the Ψ, Z space. For the body:

$$\psi = \psi_B = 0 \rightarrow \Psi_B = 0$$

At the shock

$$\psi = \psi_s = \frac{\gamma-1}{2}x \rightarrow \Psi_s = \left(\frac{\gamma-1}{2\gamma}\right)^{1/2}$$

To construct the conical form of the field equations, it is necessary to determine the transformations of the differential operators $\partial/\partial x$, $\partial/\partial\psi$, and $\partial/\partial z$ under the mapping $(x, \psi, z) \rightarrow (x^*, \Psi, Z)$, $(x^* = x)$.

We note that since $\Phi = \Phi(\Psi, Z)$, $\partial\Phi/\partial x^* = 0$. Thus

$$\frac{\partial}{\partial x} = \frac{\partial}{\partial x} - \frac{\Psi}{x}\frac{\partial}{\partial \Psi} - \frac{Z}{x}\frac{\partial}{\partial Z} \tag{47a}$$

$$x^2\frac{\partial^2}{\partial x^2} = \Psi^2\frac{\partial^2}{\partial \Psi^2} + 2\Psi Z\frac{\partial^2}{\partial \Psi \partial Z} + Z^2\frac{\partial^2}{\partial Z^2} + 2\Psi\frac{\partial}{\partial \Psi} + 2Z\frac{\partial}{\partial Z} \tag{47b}$$

$$\frac{\partial}{\partial \psi} = -\frac{1}{cx}\frac{\partial}{\partial \Psi} \tag{47c}$$

$$\frac{\partial^2}{\partial \psi^2} = \frac{1}{c^2x^2}\frac{\partial^2}{\partial \Psi^2} \tag{47d}$$

$$\frac{\partial}{\partial z} = -\frac{1}{cx}\frac{\partial}{\partial Z} \tag{47e}$$

$$c^2x^2\frac{\partial^2}{\partial z^2} = \frac{\partial^2}{\partial Z^2} \tag{47f}$$

Hence, the conical form of equation 42 becomes:

$$L[p] \equiv \{(\Psi^2-1)\frac{\partial^2}{\partial \Psi^2} + 2\Psi Z\frac{\partial^2}{\partial \Psi \partial Z} + (Z^2-1)\frac{\partial^2}{\partial Z^2} + 2\Psi\frac{\partial}{\partial \Psi} + 2Z\frac{\partial}{\partial Z}\}p = 0 \tag{48}$$

It is noted that v and w obey inhomogeneous wave equations; and hence, we expect that their conical forms are inhomogeneous modifications of equation 48. A study of the regions for which the characteristics of equation 48 are real gives the result that the unit circle $\Psi^2 + Z^2 = 1$ is a P line for that equation, i.e., the equation is elliptic inside this circle and hyperbolic outside of it.

For purposes of formulation of the elliptic boundary value problem

for p, it will be necessary to obtain its derivatives leading out of the shock. In accordance with this, the system, 38 and the boundary conditions, 41 will now be reduced using the fact that the dependent variables exhibit the conical invariance, 44. Thus, equations 47 and 38 imply:

$$\left.\begin{aligned} &[(\gamma-1)/2\gamma]^{1/2}[\Psi p_{\Psi} + Z p_Z] - v_{\Psi} - w_Z = 0 && (49a)\\ &[(\gamma-1)/2\gamma]^{1/2} p_{\Psi} - \Psi v_{\Psi} - Z v_Z = 0 && (49b)\\ &[(\gamma-1)/2\gamma]^{1/2} p_Z - \Psi w_{\Psi} - Z w_Z = 0 && (49c) \end{aligned}\right\}$$

Proceeding next to the evaluation of the boundary conditions, we note that $v(x, 0, z) \equiv v(0, Z) = \operatorname{sgn} z = \operatorname{sgn} Z = v_B$ where we have here, as before, limited our considerations to the profile for which $f = \operatorname{sgn} z$.

At the shock we obtain:

$$p_s = 2v_s = p\{[(\gamma-1)/2\gamma]^{1/2}, Z\} = \frac{4}{\gamma+1} g_x \qquad (50a)$$

$$= \frac{4}{\gamma+1} \frac{\partial}{\partial x}[xG(Z)] = \frac{4}{\gamma+1}[G - ZG']$$

$$w_s = -\frac{G'(Z)}{c} \qquad (50b)$$

As suggested previously, the mode of solution of the system, 49 and boundary conditions, 50 for the three-dimensional region, i. e., $w \neq 0$, (inside MPQTM in figure 2) will be to solve a boundary value problem for p and determine v and w from the solutions of the equations of the system using the p solution as a known right-hand side.

To complete the formulation of the p problem it will be necessary to determine its value on certain portions of the Mach circle,

i. e., QT and PM, shown in figure 2. In addition, the value of p_Ψ on TM and QP will be used.

The P line values for p will be obtained by determining the hyperbolic region conditions. For this domain, a constant state solution satisfies the equations and boundary conditions. Since the flow is two-dimensional, w = 0. Also by the boundary condition at the body:

$$v = v_B = \text{sgn } z = v_s = \frac{2}{\gamma+1} g_x \tag{51}$$

Integrating 51:

$$g = \frac{\gamma+1}{2} \times \text{sgn } z + \text{constant}$$

Since the shock perturbation surface will be assumed attached at the leading edge, we have:

$$g = \frac{\gamma+1}{2} \text{ x sgn } z$$

Finally, since $p_s = 2v_s = 2 \text{ sgn } z$

$$p = p_s = 2 \text{ sgn } z$$

Summarizing, in the hyperbolic region, the solution is:

$$v = \text{sgn } z \tag{52a}$$

$$p = 2 \text{ sgn } z \tag{52b}$$

$$w = 0 \tag{52c}$$

$$g = \frac{\gamma+1}{2} \text{ x sgn } z \tag{52d}$$

Next, the desired values of p_Ψ will be determined from the equations 49 and 50. From equation 49b specialized to the body, $\Psi = 0$, there results:

$$\{[(\gamma-1)/2\gamma]^{1/2} p_\Psi - Z v_Z\}_B - \lim_{\Psi \to 0} \Psi v_\Psi = 0$$

Now, it will be assumed that v is sufficiently well behaved to allow

$$\Psi v_\Psi \to 0 \quad \text{as} \quad \Psi \to 0$$

Furthermore, since:

$$v_B = v(0, Z) = 0$$

$$\frac{\partial v}{\partial Z}\bigg|_{\Psi=0} = 0 = \frac{dv_B}{dZ}$$

Hence

$$\frac{\partial p}{\partial \Psi}\bigg|_{\Psi=0} = 0$$

Proceeding to the determination of $p_\Psi\big|_s \equiv p_\Psi\big|_{\Psi=\Psi_s}$, we note that since Ψ_s = constant and

$$\frac{d\Psi}{dZ} = \frac{\partial \Phi}{\partial \Psi}\bigg|_s \frac{d\Psi_s}{dZ} + \frac{\partial \Phi}{\partial Z}\bigg|_s \tag{53}$$

where

$$\Phi = (p, v, w)$$

then:

$$\frac{d\Psi_s}{dZ} = 0 \tag{54}$$

and hence:

$$\frac{d\Phi_s}{dZ} = \frac{\partial \Phi}{\partial Z}\bigg|_s \tag{55}$$

Substitution of equation 55 into the shock conditions 50 gives:

$$p_Z\big|_s = -\frac{4ZG''(Z)}{\gamma+1} \tag{56a}$$

$$w_Z\big|_s = -\frac{G''}{c} \tag{56b}$$

$$v_Z\big|_s = -\frac{2Z}{\gamma+1} G'' \tag{56c}$$

Further substitution of equation 56 into equations 49a and 49b gives the following system for the unknowns $p_\Psi\big|_s$ and $v_\Psi\big|_s$:

$$\left.\begin{aligned} -\frac{\gamma-1}{2\gamma} p_\Psi\big|_s + v_\Psi\big|_s &= \left(1 - \frac{4Z^2}{\gamma(\gamma+1)c^2}\right) cG'' \\ p_\Psi\big|_s - v_\Psi\big|_s &= -\frac{4cZ^2G''}{(\gamma-1)(\gamma+1)} \end{aligned}\right\} \tag{57}$$

Using $c = [\gamma(\gamma-1)/2]^{1/2}$, and solving, we get

$$p_\Psi\big|_s = \frac{[8\gamma/(\gamma-1)]^{1/2}}{\gamma+1}\left[1 - \frac{2(2\gamma-1)}{\gamma+1} Z^2\right] G'' \tag{58}$$

Hence

$$G'' = \frac{p_\Psi\big|_s}{a+bZ^2} = \frac{p_Z\big|_s}{-\frac{4}{\gamma+1} Z} \tag{59}$$

or:

$$\frac{4}{\gamma+1} Z p_\Psi\big|_s + (a + bZ^2) p_Z\big|_s = 0 \tag{60}$$

where:

$$a \equiv \frac{1}{\gamma+1}\left(\frac{8\gamma}{\gamma-1}\right)^{1/2} \tag{61a}$$

$$b \equiv -4\left(\frac{2\gamma}{\gamma-1}\right)^{1/2}\frac{2\gamma-1}{(\gamma+1)^2} \tag{61b}$$

Thus, the unknown shock shape function has been eliminated from the problem on the basis of the equalities in 54. In place of 54, the condition, 60 specifies the value of the oblique derivative of p.

To obtain a symmetrical formulation of the p problem, we note that if:

$$p(\Psi, Z) = p(-\Psi, Z)$$

with p having the required continuity properties, the boundary condition $p_\Psi\big|_{\Psi=0} = 0$ is automatically satisfied. Accordingly, the final form of the problem is as indicated in figure 3.

The operator L may now be reduced to the Laplacian by means of the well-known Tschaplygin transformation. This mapping is used in conical supersonic flow and is discussed thoroughly in references 4 and 5.

Accordingly, if we introduce the polar coordinates:

$$\Psi = R \sin\theta$$

$$Z = R \cos\theta$$

Then:

$$L = (R^2-1)\frac{\partial}{\partial R^2} + \left(2R - \frac{1}{R}\right)\frac{\partial}{\partial R} - \frac{1}{R^2}\frac{\partial^2}{\partial\theta^2}$$

and the Tschaplygin's transformation given by:

$$s = \frac{1 - (1-R^2)^{1/2}}{R} \tag{62a}$$

$$\varphi = \theta \tag{62b}$$

maps L into

$$\Delta = \frac{\partial^2}{\partial s^2} + \frac{1}{s}\frac{\partial}{\partial s} + \frac{1}{s^2}\frac{\partial^2}{\partial \theta^2}$$

The mapping, 62 can be written more compactly if the complex variables defined as:

$$\zeta = Re^{i\theta}$$

$$\epsilon = se^{i\varphi}$$

are introduced. Thus, 62 can be expressed as:

$$\zeta = \frac{2\epsilon}{1 + |\epsilon|^2} \tag{63a}$$

$$\epsilon = \frac{1 - (1 - |\zeta|^2)^{1/2}}{\overline{\zeta}} \tag{63b}$$

A geometric interpretation of the Tschaplygin transformation can be made by referring to figures 4a and 4b. Figure 4a depicts the projection on a unit sphere of point E contained in the plane P. The polar coordinates in P of this point correspond respectively to the modulus and argument of the complex variable ζ. From E, a line is projected perpendicular to the plane P intersecting at D, a unit sphere tangent to P at its south pole A. Hence, C, the intersection of the line BD with the plane P is the stereographic projection of the point D, from the Riemann Sphere, and as such, defines the vector AC. The

magnitude of AC will be shown to be equal to the modulus of the complex variable, ϵ. This can be accomplished by reference to figure 4b, where a meridional cut is depicted. It is apparent that argument of ζ is preserved in the transformation, and hence, the mapping corresponds merely to a stretching of all position vectors. By the proportionality of the sides of the similar triangles BAC and EDC, the following relation is obtained:

$$\frac{2}{2s} = \frac{1 - (1 - R^2)^{1/2}}{2s - R}$$

Solving:

$$s = \frac{1 - (1 - R^2)^{1/2}}{R}$$

as was to be shown.

The stereographic interpretation will be found to facilitate rapid visualization of the correspondence between regions in the $\zeta \rightarrow \epsilon$ mapping. Specifically, we will be concerned with the region PQRS and its boundaries as shown in figure 5. In the ζ plane, PQRS is formed by arcs of the lines, $|\zeta| = 1$ and $\Psi = \pm[(\gamma-1)/2\gamma]^{1/2}$. From the stereographic model, it can be deduced immediately that the transformation leaves the unit circle invariant. It is also readily apparent that the interior of the region bounded by $|\zeta| = 1$ maps in a one-to-one manner into the interior of $|\epsilon| = 1$. Also under 63, the region $\text{Im } \zeta \leq [(\gamma-1)/2\gamma]^{1/2}$ maps into the annular domain, $|\epsilon - i[2\gamma/(\gamma-1)]^{1/2}| \geq [(\gamma+1)/(\gamma-1)]^{1/2}$ and similarly, $\text{Im } \zeta \leq -[(\gamma-1)/2\gamma]^{1/2}$ maps into $|\epsilon + i[2\gamma/(\gamma-1)]^{1/2}| \geq [(\gamma+1)/(\gamma-1)]^{1/2}$. Since

$$\text{Im } \zeta,\ \text{Re } \zeta \gtrless 0 \longleftrightarrow \text{Im } \epsilon,\ \text{Re } \epsilon \gtrless 0$$

the points, P, Q, R and S have their relative orientation preserved in the mapping.

On the basis of the foregoing information, the correspondence between regions and boundaries in both planes is as shown in figure 5, where similarly shaded regions are mappings of each other. The boundaries in the ϵ plane now appear as a series of arcs from a system of mutually orthogonal circles. Because of this orthogonality, it is possible to imbed these boundaries into a bipolar network; or equivalently, map them into a rectangle. Rather than dealing with eigenfunction expansions based on the bipolar separation solutions, and tailoring them to fit the conditions on the rather complicated curved boundaries, a conformal transformation will be sought to change the boundaries into the rectangular shape. The nature of this mapping becomes evident when certain representations are obtained for the bipolar circles. Specifically, we envision a network of circles:

$$\text{mod}\left(\frac{\epsilon-i}{\epsilon+i}\right) = \text{const.} \equiv \xi \tag{64a}$$

and another family described by:

$$\arg\left(\frac{\epsilon-i}{\epsilon+i}\right) = \text{const.} \equiv \eta \tag{64b}$$

That these two families are orthogonal trajectories of one another can be seen from the bilinear transformation:

$$\tau = \frac{\epsilon-i}{\epsilon+i} \tag{65}$$

Under 65, the ξ circles map into circles concentric with the origin of the ζ plane. The η family maps into a bundle of rays emanating from the origin, obviously orthogonal to the circles.

The circular arcs comprising the boundary PQRS shown in the ϵ plane in figure 5 will now be represented in the form of equation 65. For the circle containing the arc PVQ, the form 64a is appropriate, since the poles are not on the circumference. Accordingly:

$$\text{mod } \frac{\epsilon - i}{\epsilon + i} = \xi_o = \text{mod } \left(\frac{\epsilon_T - i}{\epsilon_T + i} \right) \tag{66}$$

where

$$\epsilon_T = \left[2\gamma/(\gamma-1) \right]^{1/2} - \left[(\gamma+1)/(\gamma-1) \right]^{1/2}$$

Therefore:

$$\xi_o = \left(\frac{\left[(2\gamma/(\gamma-1)) \right]^{1/2} - 1}{\left[2\gamma/(\gamma-1) \right]^{1/2} + 1} \right)^{1/2} \tag{67}$$

Similarly, for the circle containing the arc RUS:

$$\xi = 1/\xi_o \tag{68}$$

The remaining portion of the boundary which is the unit circle passes through the poles. Hence, it is a member of the family 64b. η shifts by π as we move from the right half plane to the left. This is shown by reference to figure 6, where a circumferential point in the right-hand half plane is depicted. From the notation on the figure:

$$-\alpha = \arg (\epsilon - i), \quad \beta = \arg (\epsilon + i)$$

Since

$$\alpha + \beta = \pi/2$$

$$\arg \frac{\epsilon - i}{\epsilon + i} = -\frac{\pi}{2}$$

Similarly, referring to figure 6b we obtain:

$$\alpha = \arg\ i - \epsilon$$

$$\beta = \arg\ -i - \epsilon$$

And since:

$$\alpha + \beta = \pi/2$$

$$\arg \frac{\epsilon - i}{\epsilon + i} = \frac{\pi}{2}$$

As a result of the foregoing, the boundaries in question will map into a semi-annular shape in the τ plane. Furthermore, the transformation

$$\nu = \ln\ -\tau$$

will transform these boundaries into the desired rectangular shape, since here:

$$\text{Re}\ \nu = \ln \text{ mod } -\tau = \ln \xi$$

$$\text{Im}\ \nu = \arg\ -\tau = -\eta$$

The shaded correspondence shown between figure 7 and figure 5 is deduced from the conformality property of the mapping, i. e., corresponding regions lie on the left-hand side of an observer making counter-clockwise circuits around corresponding boundaries in each of the ϵ and ν planes.

By way of summary, then, the transformations:

$$\zeta = \frac{2\epsilon}{1 + |\epsilon|^2} \tag{63a}$$

$$\nu = \ln \frac{i - \epsilon}{i + \epsilon} \tag{69}$$

have enabled us to simplify the rather general elliptic operator and

boundaries of the p problem as formulated in the ζ plane. This has been accomplished in two ways; the elliptic operator, L of equation 48 is reduced to the Laplacian, and the original segment shaped region is now rectangular in appearance.

Despite this tremendous simplification, the transformation of the boundary conditions into a reasonably compact form under the combined transformation $\zeta \rightarrow \nu$ would seem rather improbable due to the somewhat complicated nature of the mappings. Surprisingly, this is not the case, as will now be shown.

For this purpose, the mappings between the real and imaginary components of ζ and ν will first be determined. Accordingly, the inverse of 69 is:

$$\epsilon = i \frac{1 - e^{\nu}}{1 + e^{\nu}} \tag{70}$$

Substitution for ϵ from equation 70 into equation 63a gives:

$$\zeta = \frac{2i(1 - e^{\nu})(1 + \overline{e^{\nu}})}{|1 + e^{\nu}|^2 + |1 - e^{\nu}|^2}$$

Now if:

$$\nu = \sigma + i\mu$$

we obtain after some manipulation:

$$\zeta = \frac{2e^{\sigma} \sin \mu + i[1 - e^{2\sigma}]}{1 + e^{2\sigma}}$$

Hence, by equating reals and imaginaries, we obtain finally:

$$\Psi = - \text{th } \sigma \ , \quad Z = \sin \mu \ \text{sech } \sigma \tag{71a, b}$$

With equations 71, it is now possible to compute the transformation of the oblique derivative condition, 60, under the mapping $\zeta \rightarrow \nu$. Accordingly, the partial derivative operators are mapped as follows:

$$\frac{\partial}{\partial \sigma} = - \operatorname{sech}^2 \sigma \frac{\partial}{\partial \Psi} - \operatorname{sech} \sigma \operatorname{th} \sigma \sin \mu \frac{\partial}{\partial Z} \tag{72a}$$

$$\frac{\partial}{\partial \mu} = \cos \mu \operatorname{sech} \sigma \frac{\partial}{\partial Z} \tag{72b}$$

or

$$- \frac{\partial}{\partial \Psi} = \operatorname{ch}^2 \sigma \frac{\partial}{\partial \sigma} + \operatorname{sh} \sigma \operatorname{ch} \sigma \tan \mu \frac{\partial}{\partial \mu} \tag{73a}$$

$$\frac{\partial}{\partial Z} = \sec \mu \operatorname{ch} \sigma \frac{\partial}{\partial \mu} \tag{73b}$$

Now:

$$\sigma_o = - \operatorname{th}^{-1} [(\gamma-1)/2\gamma]^{1/2} \tag{74}$$

Also:

$$\Phi_s = \Phi(\sigma_o, \mu), \quad [\Phi = p_\sigma, p_\mu] \tag{75}$$

$$\operatorname{sh} \sigma_o = - [(\gamma-1)/(\gamma+1)]^{1/2} \tag{76}$$

$$\operatorname{ch} \sigma_o = [2\gamma/(\gamma+1)]^{1/2} \tag{77}$$

Substitution for the appropriate quantities from equations 73, 74, 75, 76 and 77 into equation 60 gives the following condition for the oblique derivative of p at the shock.

$$p_\sigma \big|_s - [\gamma/2(\gamma-1)]^{1/2} \operatorname{ctn} \mu \, p_\mu \big|_s = 0 \tag{78}$$

Next, the condition on the normal derivative at the body will be considered. The body line $\Psi = 0$ maps into the line $\sigma = 0$. Assuming that:

$$\text{sh } \sigma \tan \mu \, p_\mu \to 0 \quad \text{as} \quad \sigma \to 0 \quad \text{for} \quad |\mu| < \frac{\pi}{2}$$

we obtain

$$\left.\frac{\partial p}{\partial n}\right|_B \equiv p_\psi(0, Z) = 0 \longleftrightarrow p_\sigma[0, \mu] = 0$$

Since:

$$p(\sigma, \pm \frac{\pi}{2}) = \pm 2, \quad |\sigma| < |\sigma_o|$$

the condition that $p_\sigma[0, \mu] = 0$ can be satisfied, if p is made an even function of σ. We now investigate the member of the class of (p, v, w) solutions which evolves under the assumptions that:

(i) p is regular in the elliptic domain and on its boundaries,

(ii) p is unique.

Since the boundary is rectangular in the v plane, the σ, μ coordinates are separable, i.e., solutions of the following form can be tailored to the boundary conditions:

$$p = \frac{4\mu}{\pi} - \sum_{n=1}^{\infty} A_n \text{ ch } 2n\sigma \sin 2n\mu \tag{79}$$

The A_n's will be determined from a direct substitution of equation 79 into 78. Accordingly, we find

$$[2\gamma/(\gamma-1)]^{1/2} \text{ctn } \mu \left\{\frac{2}{\pi} - \sum_{n=1}^{\infty} nA_n \text{ ch } 2n\sigma_o \cos 2n\mu\right\}$$
$$= -\sum_{n=1}^{\infty} 2nA_n \text{ sh } 2n\sigma_o \sin 2n\mu \tag{80}$$

If we set:

$$B \equiv [\, 2\gamma/(\gamma-1)]^{1/2} \tag{81}$$

$$B_n \equiv nA_n \tag{82}$$

then it follows that:

$$\frac{2B}{\pi}\cos\mu = \sum_{n-1}^{\infty} B_n\{[\frac{B}{2}\,\mathrm{ch}\,2n\sigma_o + \mathrm{sh}\,2n\sigma_o][\cos(2n+1)\mu]$$

$$+ [\frac{B}{2}\,\mathrm{ch}\,2n\sigma_o - \mathrm{sh}\,2n\sigma_o][\cos(2n-1)\mu]\}$$

letting:

$$2n + 1 = 2m - 1$$

or:

$$n = m - 1, \quad m = n + 1$$

we have

$$\frac{2B}{\pi}\cos\mu = \sum_{m=2}^{\infty} B_{m-1}[\frac{B}{2}\mathrm{ch}\,2(m-1)\sigma_o + \mathrm{sh}\,2(m-1)\sigma_o]\cos(2m-1)\mu$$

$$+ \sum_{n-1}^{\infty} B_n[\frac{B}{2}\,\mathrm{ch}\,2n\sigma_o - \mathrm{sh}\,2n\sigma_o]\cos(2n-1)\mu$$

implying:

$$B_1 = \frac{2B/\pi}{\frac{B}{2}\,\mathrm{ch}\,2\sigma_o - \mathrm{sh}\,2\sigma_o} \tag{83}$$

and the following two-term recursion relation for $n = 2, 3, 4, \ldots$

$$-\frac{B_n}{B_{n-1}} = \frac{\frac{B}{2}\,\mathrm{ch}\,2(n-1)\sigma_o + \mathrm{sh}\,2(n-1)\sigma_o}{\frac{B}{2}\,\mathrm{ch}\,2n\sigma_o - \mathrm{sh}\,2n\sigma_o} \tag{84}$$

the solution of which is:

$$\frac{B_n}{B_1} = \prod_{k=2}^{n} \frac{B_k}{B_{k-1}} \tag{85}$$

The convergence of the Fourier series for p, (79), will next be determined. To expedite this process, it will be necessary to form an asymptotic representation for B_n/B_{n-1} from equation 84 as $n \to \infty$. This can be easily computed to be:

$$\frac{B_n}{B_{n-1}} \doteq \frac{\frac{B}{2} - 1}{\frac{B}{2} + 1} \; e^{-2|\sigma_o|}$$

$$= \frac{1 - [2(\gamma-1)/\gamma]^{1/2}}{1 + [2(\gamma-1)/\gamma]^{1/2}} \cdot \frac{1 - [(\gamma-1)/2\gamma]^{1/2}}{1 + [(\gamma-1)/2\gamma]^{1/2}}$$

$$= 0.063 \quad \text{for} \quad \gamma = 7/5$$

Consider now the series

$$S = \sum_{k=1}^{n} C_k$$

where

$$C_n = 2B_n \operatorname{ch} 2n\sigma_o = e^{2n|\sigma_o|} B_n \quad \text{as} \quad n \to \infty$$

Accordingly:

$$\left| \frac{C_n}{C_{n-1}} \right| \doteq \left| \frac{1 - \frac{B}{2}}{1 + \frac{B}{2}} \right| e^{2(|\sigma_o| - |\sigma_o|)} \equiv r = \left| \frac{1 - \frac{B}{2}}{1 + \frac{B}{2}} \right|$$

That is, S is asymptotically a geometric series, having its common

ratio = r. A necessary condition for absolute convergence of the series, is that $\lim_{n \to \infty} |C_n/C_{n-1}| = r < 1$, i.e.:

$$\left| \frac{B}{2} - 1 \right| < \left| \frac{B}{2} + 1 \right|$$

This follows as a consequence of D'Alembert's ratio test. The above inequality holds for all γ. Hence, the S series is absolutely convergent. Using the comparison test, we finally deduce that the series representation for p is absolutely and uniformly convergent, verifying our original assertion, (i).

The first ten A_n's and the pressure on the body have been computed using an IBM 7090. The rapidity of convergence justifies the use of only ten terms for engineering calculations. In fact, employing any more than this number causes inconsistencies resulting from round-off errors and instabilities. Table I gives the values of these coefficients. Figures 8a and 8b show the pressure distributions.

4. 3. Calculation of the Shock Distortion Function

Proceeding toward the evaluation of the rest of the solution, we now turn our attention to the determination of the distortion function, G, which can be obtained by integration of equation 50b and the solution for p, i.e., equations 79, 83, 84 and 85 collectively. Thus

$$\frac{G}{Z} - [\gamma(\gamma+1)/2]^{1/2} = -\frac{\gamma+1}{4} \int_{-[(\gamma+1)/2\gamma]^{1/2}}^{Z} \frac{p_s(\omega)}{\omega^2} d\omega \qquad (86)$$

To facilitate the indicated quadrature, the above equation can be

re-expressed in terms of μ as the independent variable. Accordingly:

$$Z = \operatorname{sech} \sigma_o \sin \mu$$

$$dZ = \operatorname{sech} \sigma_o \cos \mu \, d\mu = [(\gamma+1)/2\gamma]^{1/2} \cos \mu \, d\mu$$

Hence:

$$G = \frac{\gamma+1}{2} \sin \mu \left[1 - \frac{1}{2} \int_{-\pi/2}^{\mu} \frac{p_s(\tau) \cos \tau}{\sin^2 \tau} \, d\tau \right] \tag{87a}$$

where:

$$p_s(\tau) = \frac{4\tau}{\pi} - \sum_{n=1}^{\infty} A_n \operatorname{ch} 2n\sigma_o \sin 2n\tau \tag{87b}$$

Carrying out the indicated integrations, we obtain the following representation for G:

$$G^* \csc \mu = \frac{\gamma+1}{2} \left(1 - \frac{I}{2}\right) \tag{88}$$

where

$$I = \frac{4}{\pi} \left[\ln \left| \tan \frac{\mu}{2} \right| - \mu \csc \mu + \frac{\pi}{2} \right]$$

$$- \sum_{n=1}^{\infty} A_n \operatorname{ch} 2n\sigma_o \left[4n \sum_{m=0}^{n-1} \frac{\cos (2n-2m-1)\mu}{2n-2m-1} \right.$$

$$\left. - 2n \ln \left| \tan \frac{\mu}{2} \right| - \sin 2n\mu \csc \mu \right] \tag{89}$$

and:

$$G(Z) = G^*(\mu) \tag{90}$$

It can be seen immediately that 88 achieves the correct specialization to satisfy the end conditions:

$$G^*(\pm\frac{\pi}{2}) = \pm\frac{\gamma+1}{2} \tag{91}$$

since:

$$I(\pm\frac{\pi}{2}) = 0$$

Numerical calculations were made to generate the curves of G versus Z and μ shown in figures 8c and 8d for $\gamma = 7/5$. Here, it was found that numerical quadrature of the integral in equation 87a was a quicker process for machine calculation than evaluation of the rather unwieldly double series in equation 89. An interesting sidelight is the linear shape of the distortion surface over most of the interaction region for this γ value. Near the Mach cone, the shock shows a large curvature in order to effect a transition to the outlying planar sections. Subsequent analysis for $\gamma \to 1$ will show that this transition region shrinks to a point, i. e., the shock surface consists of three planes; and the trace of it in conical projection will show kinks at points corresponding to the intersections of these planes.

4. 4. Evaluation of the Velocities

To obtain the remaining portion of the solution involving the velocities v and w, we rewrite the conical system, 49, using the polar coordinates:

$$\Psi = R \sin\theta \tag{92a}$$

$$Z = R \cos\theta \tag{92b}$$

as independent variables. Accordingly:

$$\frac{R}{B}\frac{\partial p}{\partial R} - (\sin\theta\frac{\partial}{\partial R} + \frac{\cos\theta}{R}\frac{\partial}{\partial\theta})v - (\cos\theta\frac{\partial}{\partial R} - \frac{\sin\theta}{R}\frac{\partial}{\partial\theta})w = 0 \qquad (93a)$$

$$R\frac{\partial v}{\partial R} = \frac{1}{B}[\sin\theta\frac{\partial}{\partial R} + \frac{\cos\theta}{R}\frac{\partial}{\partial\theta}]p = \frac{p_\Psi}{B} \qquad (93b)$$

$$R\frac{\partial w}{\partial R} = \frac{1}{B}[\cos\theta\frac{\partial}{\partial R} - \frac{\sin\theta}{R}\frac{\partial}{\partial\theta}]p = \frac{p_Z}{B} \qquad (93c)$$

Integrating along a ray θ = constant from the point (R, θ) to the boundary point, $[R_B(\theta), \theta]$ we obtain from equations 93b and 93c the solutions:

$$v(R, \theta) = v(R_B, \theta) + \int_R^{R_B} \frac{p_\Psi(\rho, \theta)}{B\rho}\, d\rho \qquad (94a)$$

$$w(R, \theta) = w(R_B, \theta) + \int_R^{R_B} \frac{p_Z(\rho, \theta)}{B\rho}\, d\rho \qquad (94b)$$

If we define the quantities

$$\tan\theta_o = [(\gamma-1)/(\gamma+1)]^{1/2}, \quad (0 \leq \theta_o \leq \tfrac{\pi}{2})$$

$$v_B = v(R_B, \theta)$$

$$w_B = w(R_B, \theta)$$

then the following table gives the appropriate values of R_B, v_B and w_B corresponding to the indicated ranges of θ, cf. figure 9.

θ Range	R_B	v_B	w_B
$0 \leq \theta < \theta_o$	1	1	0
$\theta_o < \theta < \pi-\theta_o$	$\frac{1}{B}\csc\theta$	$\frac{1}{2}p_s \operatorname{ctn}\theta$	$-[\gamma(\gamma-1)/2]^{1/2}G'(\operatorname{ctn}\theta)$
$\pi-\theta_o < \theta \leq \pi$	1	-1	0

The above values when substituted into equations 94a and 94b give solutions corresponding to the indicated regions. The complexity of the integrands has thus far prevented further reduction of the velocity formulae.

In certain numerical applications, a series representation of v and w may be desired rather than the integral formulae. The singular behavior of these quantities would be a necessary determination prior to the calculation of such series, since their convergence would be affected in the vicinity of the singular points. To handle the foregoing possibility, the solution is tentatively written in the form:

$$\Phi = \Phi_S + \Phi_R$$

where:

Φ_S = singular part of solution

Φ_R = regular part of solution in the form of a Fourier series

Heuristically, we suspect that v and w both have the origin as their only singular point, a conclusion more or less intuitively based on the nature of the boundary conditions and the underlying equations.

Using the solution for p it can be shown that as $R \to 0$:

$$p = \kappa_1 R \cos\theta + O(R^3) \tag{95a}$$

$$p_Z = \kappa_1 + O(R^2) \tag{95b}$$

$$p_\Psi = \kappa_2 R^2 \cos\theta \sin\theta = \kappa_2 \frac{R^2}{2} \sin 2\theta + O(R^4) \tag{95c}$$

where:

$$\kappa_1 = \frac{4}{\pi} - 2\sum_{n=1}^{\infty} B_n, \quad \kappa_2 = \frac{4}{\pi} - \sum_{n=1}^{\infty} (8n^2+2)B_n$$

Substitution of equation 95 into equations 93b and 93c gives:

$$R \frac{\partial v}{\partial R} = O(R^2)$$

$$R \frac{\partial w}{\partial R} = \frac{K_1}{B} + O(R^2)$$

Integration gives the following singular representations of the velocities:

$$v = V(\theta) + O(R^2) \tag{96a}$$

$$w = \frac{K_1}{B} \ln R + W(\theta) + O(R^2) \tag{96b}$$

5. A Related Problem in Linear Supersonic Flow

To compare the results given above with an analogous linear flow, we study the configuration shown in figure 10 at low supersonic Mach numbers, i. e. such that $M_\infty \delta \ll 1$. Here, the deviation of the sections is about the $\bar{x}, \bar{z}$ plane rather than a wedge as occurred in the HSD case. Moreover, the flow deflection is of $O(\delta)$ rather than $O(\delta\epsilon)$ as occurs in the HSD regime. Despite these differences, the configurations are similar, if y is thought of as playing the role of ψ in the HSD case. A precise application of the HSD geometry to linear flow would involve second order linearized theory, and has not been attempted in the present work. Physically, the vortical effects of the entropy gradients arising from the shock wave difraction about the $\bar{x}$ axis, resulting from interaction with the Prandtl-Meyer expansion region are negligible, since the entropy changes and consequently the vorticity are at most $O(\delta^3)$. The implications of this fact are that the flow is to all intents and purposes irrotational, and the velocity components must be compatible with the

fact that they comprise a solenoidal vector. The other connotations of the linearized flow have already been discussed in the introduction.

Since the linear problem has been treated extensively in the literature, e. g. reference 4, only a summary of the related mathematical problem and its solution will be given here.

Accordingly, the equations of motion and boundary conditions of the linear case are compared with those for the HSD configuration in Table II. Here, the differences in the constants reflect normalizations and are not essential to understanding the conceptual similarity in appearance of the formulations, the motivating idea in both frameworks consisting of the notions of small disturbances and the fact that the streamlines are practically parallel to the x axis. Applying the procedures described in reference 4, we obtain for the solution of the linear problem shown in Table II:

$$u = \frac{4}{\beta\pi} \operatorname{Re}\{\tan^{-1}\epsilon\} = -p$$

$$v = \operatorname{Re}\left\{1 - \frac{2i}{\pi} \ln\left(\epsilon + \frac{1}{\epsilon}\right)\right\}$$

$$w = -\frac{2}{\pi} \ln|\epsilon|$$

where

$$\epsilon = \frac{1 - |(1 - |\zeta|^2)^{1/2}|}{\zeta}$$

$$\zeta = Z + iY$$

$$Z = \frac{\beta z}{x}, \quad Y = \frac{\beta y}{x}, \quad \beta = (M_\infty^2 - 1)^{1/2}$$

For the surface pressure, the above formula for p specializes to give:

$$p(0, Z) = \frac{2}{\beta\pi} \sin^{-1} Z, \quad |Z| < 1 \tag{97}$$

In terms of comparison with HSD results, it is evident from the foregoing that to within suitable normalizations and adjustment of levels, the HSD surface pressure distribution undercuts its linearized counterpart. This may be concluded from a study of figure 8a. Moreover, the characteristic non-linear peaking, a feature of the HSD distribution, is not present in the lower Mach number case.

An inspection of the formulae for the linear and HSD cases, reveals a similarity in the singular behavior at the origin for both flows. In particular, in this neighborhood, i. e., when $\epsilon, \zeta \to 0$, the representations for the linear quantities are:

$$u \doteq -\frac{2Z}{\beta\pi} + O(r^2) = -p \tag{98a}$$

$$v \doteq 1 - \frac{2\varphi}{\pi} + O(r^2) \tag{98b}$$

$$w \doteq -\frac{2}{\pi} \ln \frac{r}{2} + O(r^2) \tag{98c}$$

where:

$$r = \text{mod } \zeta$$

$$\varphi = \arg \zeta$$

Comparing equations 98 with equations 95a and 96, we conclude that the linear and HSD solutions show similarities in their singular character near the origin.

III. A NEWTONIAN PERTURBATION APPROXIMATION

1. Lateral Interaction Theory for General Perturbations

In this section, we consider the effect of allowing the specific heat ratio, γ, of the HSD flow in II to approach one. Since a large degree of simplification is anticipated, the general non-conical profile is treated. That is, the body is expressed as:

$$B = \bar{y} - \delta\left[\bar{x} + \epsilon f\left(\bar{x}, \frac{\bar{z}}{b}\right)\right] = 0 \qquad (99)$$

where the notation of II is used.

The significant parameters will be taken to be ϵ and λ, where

$$\lambda \equiv \frac{\gamma-1}{\gamma+1} \rightarrow \gamma = 1 + 2\lambda \quad \text{as} \quad \lambda \rightarrow 0 \qquad (100)$$

$1/\lambda$ represents the limiting density ratio immediately behind the shock wave as the free stream Mach number tends to infinity. It will be found somewhat more convenient to use this parameter than other choices involving the difference of γ and 1.

The following three limits are possible as $\gamma \rightarrow 1$:

(i) $\frac{\epsilon}{\lambda} \rightarrow 0$

(ii) $\frac{\epsilon}{\lambda} = O(1)$ as $\lambda \rightarrow 0$

(iii) $\frac{\epsilon}{\lambda} \rightarrow \infty$

Here, we will consider only (i), since it permits the boundary conditions to be satisfied on the undisturbed surfaces, a fact which can easily be demonstrated from a consideration of the relative orders of the coordi-

nates of disturbed and undisturbed boundaries. Effectively we study the $(\gamma-1)$ dependence of our previous $(\epsilon \to 0)$ perturbation solution.

The HSD equations and boundary conditions written in terms of the density parameter, λ are:

$$\left.\begin{aligned} p_x + v_\psi + w_z &= 0 \qquad (101a)\\ \lambda p_\psi + v_x &= 0 \qquad (101b)\\ \lambda p_z + w_x &= 0 \qquad (101c)\end{aligned}\right\}$$

$$v_B = v(x, 0, z) = f_x \qquad (102a)$$

$$p_s = 2v_s = p(x, \lambda x, z) = 2g_x \qquad (102b)$$

$$w_s = -g_z \qquad (102c)$$

Equations (101) are hyperbolic, having as one set of characteristics the Mach cones:

$$\psi^2 + z^2 - \lambda x^2 = 0$$

According to theory of hyperbolic systems, the domain of dependence of a field point P consists of the regions of intersection of the Mach forecone emanating from P and the unperturbed shock and body.

We now restrict our considerations to those bodies which produce shock distortions having lateral wave lengths, b, which scale as the forecone apex angle, $\sqrt{\lambda}\,\delta$ as $\lambda \to 0$. An example of such a shape is the differential panel configuration treated in II.

Noting furthermore that the dihedral angle between the undistorted shock and body is of $O(\lambda)$ as $\lambda \to 0$, we conclude that the coordinate distortions:

$$x^* = x, \quad \lambda\psi^* = \psi, \quad \sqrt{\lambda}\, z^* = z \tag{103}$$

preserve the similarity of the domain of dependence of P in the limit (i). A study of equations 102 leads us to postulate the following asymptotic expansions for the flow quantities, valid as $\lambda \to 0$:

$$p(x, \psi, z; \gamma) = p^*(x^*, \psi^*, z^*) + \ldots \tag{104a}$$

$$v(x, \psi, z; \gamma) = v^*(x^*, \psi^*, z^*) + \ldots \tag{104b}$$

$$w(x, \psi, z; \gamma) = \frac{1}{\sqrt{\lambda}} w^*(x^*, \psi^*, z^*) + \ldots \tag{104c}$$

$$g(x, z; \gamma) = g^*(x^*, z^*) + \ldots \tag{104d}$$

$$f(x, z) = f^*(x^*, z^*) \tag{104e}$$

The sidewash, w attains its large value as a result of the high shock slopes in the z direction resulting in turn from the similarity assumption on b. Substitution of equations 103 and 104 into equations 101 and 102 gives the following problem for the starred quantities:

$$\left.\begin{aligned} v^*_{\psi^*} + w^*_{z^*} &= 0 \qquad (105a) \\ p^*_{\psi^*} + v^*_{x^*} &= 0 \qquad (105b) \\ w^*_{x^*} &= 0 \qquad (105c) \end{aligned}\right\}$$

$$v_B = v(x, 0, z) = v^*(x^*, 0, z^*) = f^*_{x^*} \tag{106a}$$

$$p^*_s = 2v^*_s = p^*(x^*, x^*, z^*) = 2g^*_{x^*} \tag{106b}$$

$$w^*_s = -g^*_{z^*} \tag{106c}$$

Proceeding toward the determination of the solution, we first integrate equation 105c partially with respect to x from the shock to arbitrary x downstream. This gives

$$w = -g_z(\psi, z) \tag{107}$$

where the star notation has been dropped. Substitution of equation 107 into 105a gives on partial integration with respect to ψ and use of equation 106a:

$$v = f_x(x, z) + \int_0^{\psi} g_{zz}(\tilde{\psi}, z)d\tilde{\psi} \tag{108}$$

g may be now evaluated from the specialization of equation 108 at the shock, i.e. where $\psi = x$, and use of equation 106b. This gives the following integral equation for g:

$$g_x(x, z) = f_x(x, z) + \int_0^{x} g_{zz}(\tilde{\psi}, z)d\tilde{\psi} \tag{109}$$

From equation 109 it is obvious that equation 108 may be rewritten as:

$$v = f_x(x, z) + g_{\psi}(\psi, z) - f_{\psi}(\psi, z) \tag{110}$$

Substitution of equation 110 into 105a and subsequent partial integration gives:

$$p = 2g_x(x, z) + (x-\psi)f_{xx}(x, z)$$

Specializing to the body:

$$p_B = p(x, 0, z) = 2g_x(x, z) + xf_{xx}(x, z)$$

Postulating suitable restrictions on f and g, we differentiate 109 partially with respect to x to obtain the following inhomogeneous wave equation for the shock distortion function:

$$g_{xx} - g_{zz} = f_{xx}$$

Under the assumptions of attachment of the perturbation surface, as well as continuity of vertical velocity along the intersection of the shock and body at the leading edge, we obtain as initial conditions on g the relations:

$$g(0, z) = f(0, z)$$

$$g_x(0, z) = f_x(0, z)$$

The solution of this Cauchy initial value problem is obtained by reformulation of it in the following characteristic coordinates:

$$\xi = x + z$$

$$\eta = x - z$$

Upon integration in the ξ, η plane and transformation back to the (x, z) frame, we obtain finally:

$$2g = \int_{z-x}^{z} f_x[x-z+\tilde{z}, \tilde{z}]\, d\tilde{z} + \int_{z}^{z+x} f_x[x+z-\tilde{z}, \tilde{z}]\, d\tilde{z}.$$

Summary of Solution - General Perturbation

$$v = f_x(x, z) - g_\psi(\psi, z) - f_\psi(\psi, z) \qquad (110a)$$

$$w = -g_z(\psi, z) \qquad (110b)$$

$$p = 2g_x(x, z) + (x-\psi) f_{xx}(x, z) \qquad (110c)$$

$$p_B = p(x, 0, z) = xf_{xx} + \int_{z-x}^{z} \frac{\partial}{\partial(x-z+\tilde{z})} f_x[x-z+\tilde{z}, \tilde{z}]\, d\tilde{z}$$

$$+ \int_{z}^{z+x} \frac{\partial}{\partial(x-z+\tilde{z})} f_x[x+z-\tilde{z}, \tilde{z}]\, d\tilde{z} \qquad (110d)$$

$$2g = \int_{z-x}^{z} f_x[x-z+\tilde{z}, \tilde{z}]\, d\tilde{z} + \int_{z}^{z+x} f_x[x+z-\tilde{z}, \tilde{z}]\, d\tilde{z} \qquad (110e)$$

2. Specialization to Differential Flap Configuration

Applying the formulae of III. 1 to the case where

$$f = x \operatorname{sgn} z$$

we have

$$2g = \int_{z-x}^{z+x} \operatorname{sgn} \tilde{z}\, d\tilde{z} = (\operatorname{sgn} \tilde{z})\tilde{z} \Big|_{z-x}^{z+x}$$

so that finally:

$$2g = (z+x) \operatorname{sgn} (z+x) - (z-x) \operatorname{sgn} (z-x) \qquad (111a)$$

From the above expression for g we now can compute the other flow quantities. For this purpose, it is necessary to evaluate g_x and g_z. This may be accomplished by specialization of the integral formulae, or differentiation of the above expression for g. It is also necessary to note that all the functions will be defined over an open space such that the arguments of the sgn functions are never 0. This corresponds physically to the fact that the field point does not lie on either the degenerate Mach cone $x^2 - z^2 = 0$ or the surface $\psi^2 - z^2 = 0$. Thus:

$$p = \operatorname{sgn}(z + x) + \operatorname{sgn}(z - x) \tag{111b}$$

$$v = \frac{1}{2}\operatorname{sgn}(z + \psi) + \frac{1}{2}\operatorname{sgn}(z - \psi) \tag{111c}$$

$$w = \frac{1}{2}\operatorname{sgn}(z - \psi) - \frac{1}{2}\operatorname{sgn}(z + \psi) \tag{111d}$$

In order to understand the physical aspects of this flow, it will be necessary to obtain the remaining quantities, u and σ. If we assert that these variables are $O(1)$ as $\lambda \to 0$, they are governed by the following equations:

$$(u + v)_{x^*} = 0 \tag{112a}$$

$$(p - \sigma)_{x^*} = 0 \tag{112b}$$

These follow from equations 11b and 14b. Since the stagnation enthalpy is conserved everywhere, we have furthermore that

$$u_o = -1 \tag{113a}$$

and

$$u + v + \frac{p-\sigma}{2} = 0 \tag{113b}$$

Applying 113b at the shock we find that

$$u_s = - p_s \tag{114}$$

Integration of equations 112, application of equations 114, 23b and 111 gives:

$$u = - 2v \tag{115a}$$

$$\sigma = \operatorname{sgn}(z + x) + \operatorname{sgn}(z - x) - \operatorname{sgn}(z + \psi) - \operatorname{sgn}(z - \psi) \tag{115b}$$

To expedite visualization of the significance of these results, we introduce the conical coordinates:

$$\frac{\psi}{x} = \Psi \quad , \quad \frac{z}{x} = Z$$

The above solution rewritten in terms of these variables is:

$$g = xG$$

$$2G = (Z+1)\,\mathrm{sgn}\,(Z+1) - (Z-1)\,\mathrm{sgn}\,(Z-1)$$

$$p = \mathrm{sgn}\,(Z+1) + \mathrm{sgn}\,(Z-1)$$

$$-u = 2v = \mathrm{sgn}\,(Z+\Psi) + \mathrm{sgn}\,(Z-\Psi)$$

$$2w = \mathrm{sgn}\,(Z-\Psi) - \mathrm{sgn}\,(Z+\Psi)$$

$$\sigma = \mathrm{sgn}\,(Z+1) + \mathrm{sgn}\,(Z-1) - \mathrm{sgn}\,(Z+\Psi) - \mathrm{sgn}\,(Z-\Psi) = p - 2v$$

Figure 11 shows a schematic representation of the flow field. Here, the line PQ is the trace of the shock surface, the lines PM and QT are the traces of the degenerate Mach cone. The implication with respect to these traces is that they may be imagined as the projection of the pertinent boundaries in the plane $x = 1$. The flow quantities take on the indicated values in the regions shown in the figure according to the above formulae.

From an inspection of figure 11 and its three-dimensional analogue, figure 12, we see that PM and QT are very weak expansion waves; i. e., a fluid particle moving downstream (essentially along a ray through the origin) when subjected to the indicated pressure jump across these surfaces, does not accelerate correspondingly. This fact can be seen to follow as a consequence of the following momentum invariant of equations 11b, 28 and 29:

$$D\left(u + v + \frac{\gamma-1}{2}\,p\right) = 0 \qquad (116)$$

Effectively, as $\gamma \to 1$, the density of the flow becomes so large that sudden changes in the perturbation pressures are ineffective in changing the perturbation momentum. This is verified from an application of the limit (i) to equation 116 and use of equation 28c, from which we conclude that the quantity, $u + v + w$, is constant along lines parallel to the x-axis; i. e. Ψ/Z = constant lines in figure 11.

In addition, to the expansion waves present in the field of interest, it is apparent that the lines PN and NQ may be interpreted as slip surfaces since the entropy $p\text{-}\sigma$ as well as the tangential velocity perturbation are discontinuous across them. The above configuration occurs because of the interaction of the central transition shock with the outlying surfaces.

In considering the slip surfaces of the solution, we notice a mass flux across them, in direct contradiction to physical reality. This apparent paradox is explained by the fact that the mass flux arises as a result of the approximations made in the orientation of the various boundary surfaces of the problem.

As has been suggested previously, the shock shape in the degenerate three-dimensional region is:

$$G = Z \tag{117}$$

It is evident that a sidewash discontinuity exists at the points of attachment to the outlying sections

$$G = \operatorname{sgn} Z$$

As has been previously pointed out in II, figure 8d shows an

already apparent trend to the shape given by equation 117 for $\gamma = 1.4$.

3. Strip Theory

If we fail to expand the lateral coordinate suitably, the Mach forecones become straight lines parallel to the x axis in the limit (i). Hence, a point is influenced only by conditions directly upstream of it and consequently, adjacent lateral sections do not interact as in Hypersonic Strip Theory (cf. reference 1).

To illustrate, we let:

$$x^* = x, \quad \psi^* = \psi/\lambda \ , \quad z^* = z$$

Assuming:

$$p(x, \psi, z;\gamma) = p^*(x^*, \psi^*, z^*) + \ldots$$

$$v(x, \psi, z;\gamma) = v^*(x^*, \psi^*, z^*) + \ldots$$

$$w(x, \psi, z;\gamma) = w^*(x^*, \psi^*, z^*) + \ldots$$

$$f(x, z) = f^*(x^*, z^*) + \ldots$$

$$g(x, z;\gamma) = g\ (x^*, z^*) + \ldots$$

we have: (stars are dropped)

$$\left.\begin{aligned} v_\psi &= 0 \\ v_x + p_\psi &= 0 \\ w_x &= 0 \end{aligned}\right\}$$

$$v_B = v(x, 0, z) = f_x(x, z)$$

$$p_s = 2v_s = p(x, x, z) = 2g_x(x, z)$$

$$w_s = - g_z$$

The solution of which can be readily found to be:

$$p = -\psi f_{xx} + 2f_x + xf_{xx}$$

$$v = f_x(x, z)$$

$$w = -f_z(\psi, z)$$

$$g = f$$

and finally

$$p_B = p(x, 0, z) = 2f_x + xf_{xx}$$

The latter relation corresponds to the classical formula of Busemann, applied under the assumption of independence of lateral sections. Here, the first term is the slope or inelastic impact effect, and the second is the centrifugal force correction.

REFERENCES

1. Hayes, W. and Probstein, R., Hypersonic Flow Theory, Academic Press (1959).

2. Guiraud, Comptes Rendus, vol. 244, pp. 2281-2284 (1957).

3a. Holt, M. and Yim, B., "Supersonic Flow Past Finite Double Wedge Wings at Variable Thickness. Part I. Linear Variation," AFOSR TN 60-431 (1960).

3b. Holt, M. and Yim, B., "Supersonic Flow Past Finite Double Wedge Wings of Variable Thickness. Part II. Sinusoidal Variation," AFOSR TN 60-432 (1960).

4. Lagerstrom, P., "Linearized Theory of Conical Wings," NACA TN 1685 (1948).

5. Busemann, A., "Infinitesimal Conical Supersonic Flow," NACA TM 1100 (1947).

TABLE I

$A_1 = 0.63661978$

$A_2 = -0.48970751 \times 10^{-1}$

$A_3 = 0\ 26573275 \times 10^{-2}$

$A_4 = -0.13263367 \times 10^{-3}$

$A_5 = 0.67400558 \times 10^{-5}$

$A_6 = -0.35331404 \times 10^{-6}$

$A_7 = 0.19011805 \times 10^{-7}$

$A_8 = -0.10439105 \times 10^{-8}$

$A_9 = 0.58224602 \times 10^{-10}$

$A_{10} = -0.32880426 \times 10^{-11}$

TABLE II

HSDT	LINEAR
$\frac{\vec{q}}{\sigma} = \vec{i}[1 + O(\delta^2)] + j\delta(1 + \epsilon v) + \vec{k}\delta\epsilon w + \ldots$	$\frac{\vec{q}}{U} = (1 + \delta u)\vec{i} + \delta v\vec{j} + \delta w\vec{k} + \ldots$
$\frac{P-P_\infty}{\rho_\infty U^2} = \delta^2 p_o(1 + \epsilon p) + \ldots$	$\frac{P - P_\infty}{\rho_\infty U^2} = \delta p + \ldots$
$\frac{\rho}{\rho_\infty} = \sigma_o[1 + \epsilon\sigma] + \ldots$	$\frac{\rho}{\rho_\infty} = 1 + \delta\sigma + \ldots$
$\frac{p_x}{\gamma} + v_\psi + w_z = 0$	$\beta^2 p_x + v_y + w_z = 0$
$u_x + \frac{\gamma-1}{2} p_x = 0$	$u_x + p_x = 0$
$v_x + \frac{\gamma-1}{2} p_\psi = 0$	$v_x + p_y = 0$
$w_x + \frac{\gamma-1}{2} p_z = 0$	$w_x + p_z = 0$
$p_x - \gamma\sigma_x = 0$	$p_x - \frac{1}{M_\infty^2}\sigma_x = 0$
$B = \bar{y} - \delta[\bar{x} + \epsilon\ \mathrm{sgn}\ \bar{z}] = 0$	$B = y - \delta x\ \mathrm{sgn}\ z = 0$
$S = \bar{y} - \delta[\theta\bar{x} + \epsilon g(\bar{x}, \frac{\bar{z}}{b})] = 0$	$S_1 = y - \beta x = 0,\ \frac{y}{\beta x} \geq 1$
	$S_2 = x^2 - \beta^2(y^2 + z^2) = 0,\ \frac{y}{\beta x} \leq 1$

TABLE II (Continued)

HSDT	LINEAR
$v_B = v(x, 0, z) = \operatorname{sgn} z$	$v_B = v(x, 0, z) = \operatorname{sgn} z$
$p_s = 2v_s = \frac{4}{\gamma+1} g_x$	$v_s = \operatorname{sgn} z = v_M$
$= p(x, \frac{\gamma-1}{2} x, z)$	$u_M = u_s = -\frac{\delta}{\beta} \operatorname{sgn} z = -p_s = p_M$
$w_s = -g_z$	$w_s = 0 = w_M$
	(continuity across Mach cone of p, u, v, w)
$p_M = 2v_M = 2 \operatorname{sgn} z$	
$w_M = 0$	
$p_M = p(x, \pm cx\left[1 - \frac{z^2}{c^2 x^2}\right]^{1/2}, z)$	

GEOMETRY OF PROBLEM

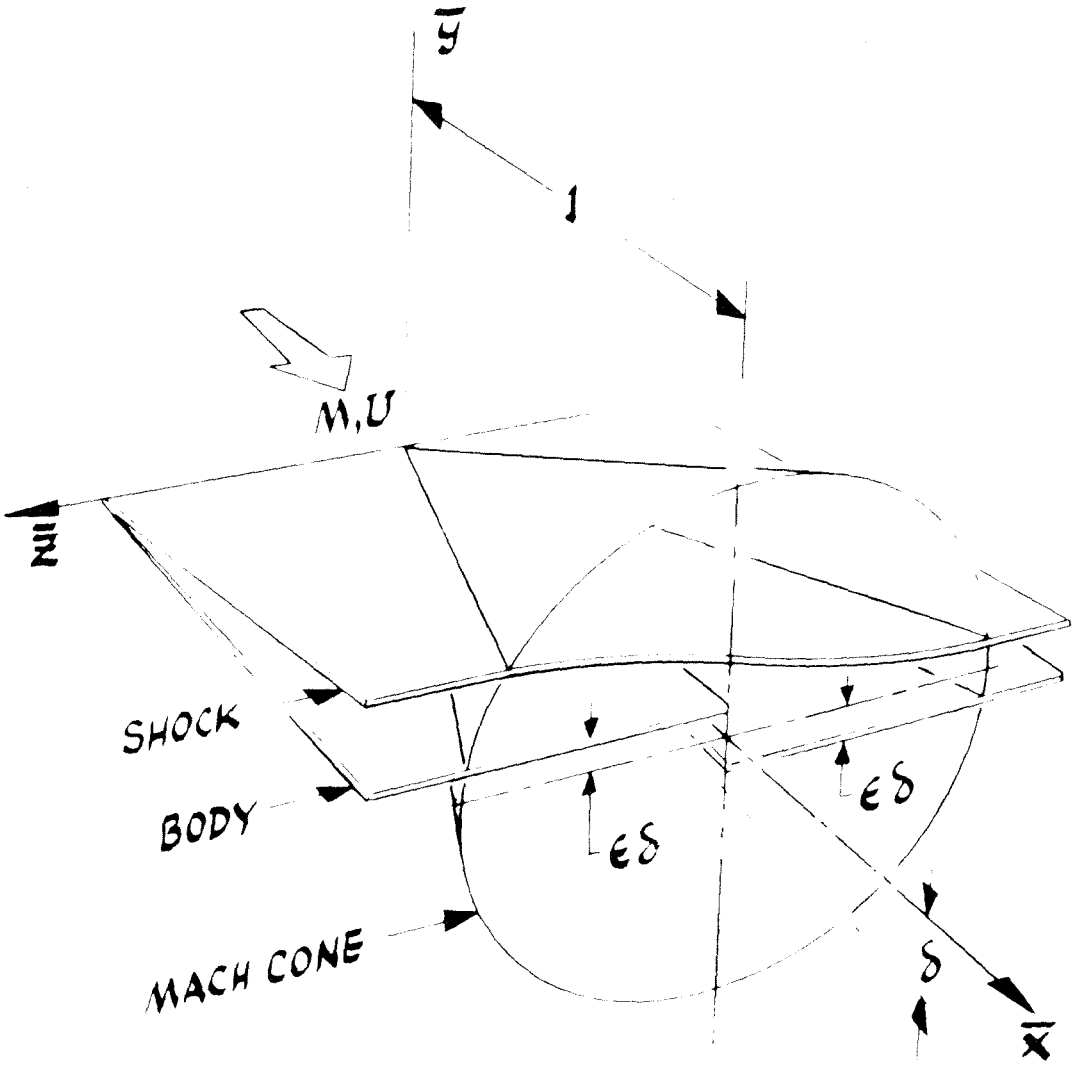

FIG 1

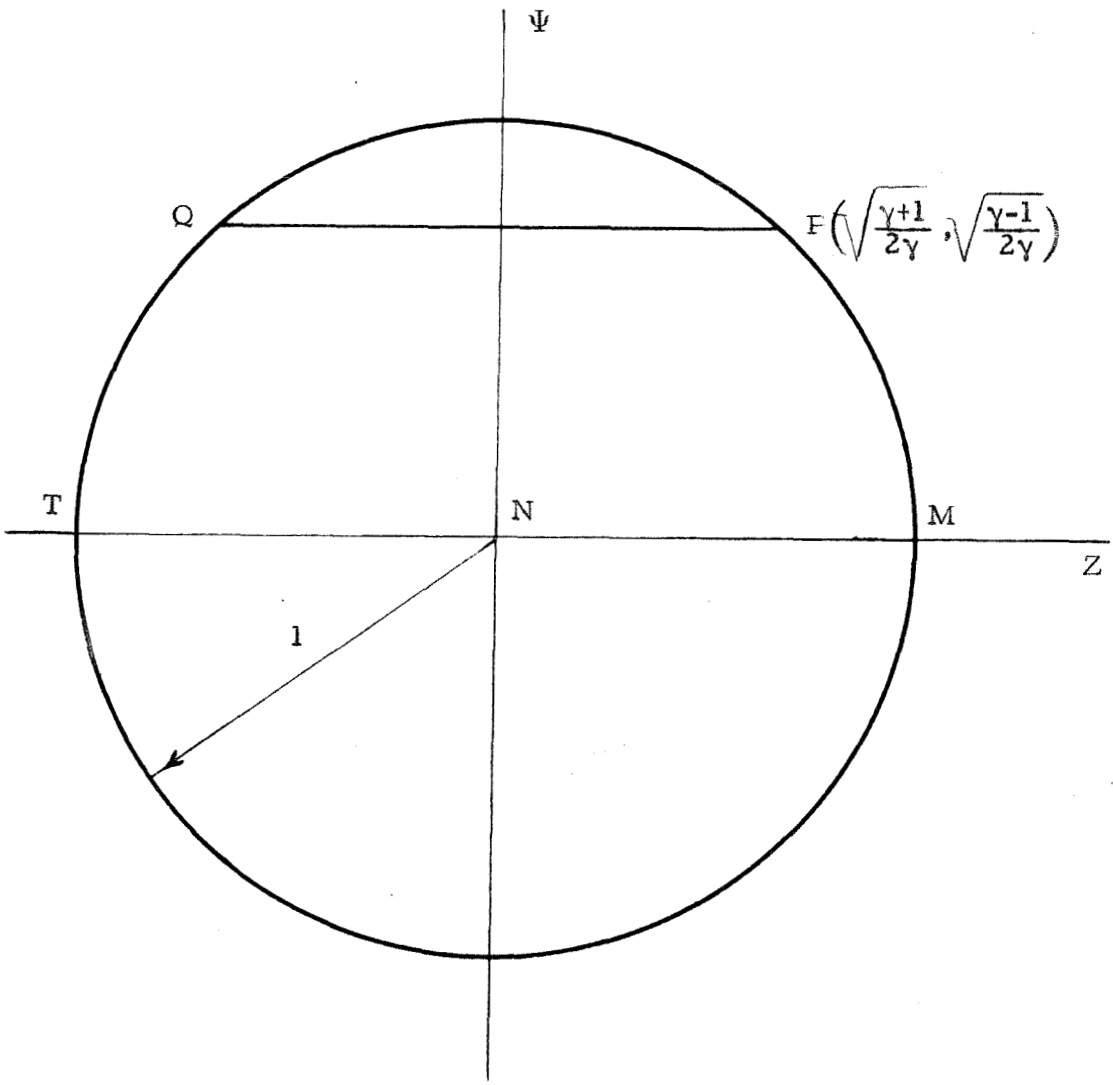
Ψ
Q
P $\left(\sqrt{\frac{\gamma+1}{2\gamma}}, \sqrt{\frac{\gamma-1}{2\gamma}}\right)$
T
N
M
Z
1

FIGURE 2

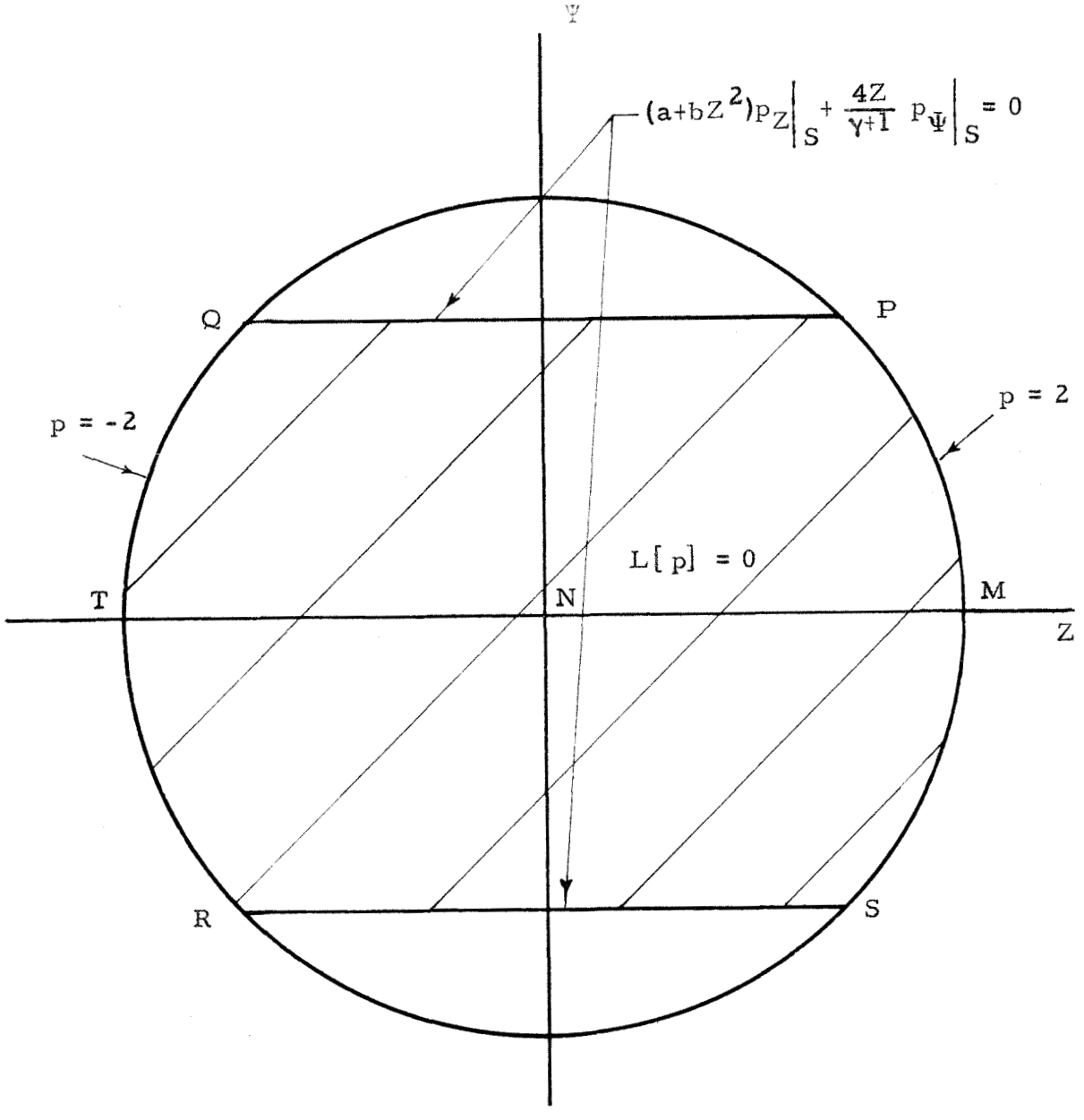

FIGURE 3

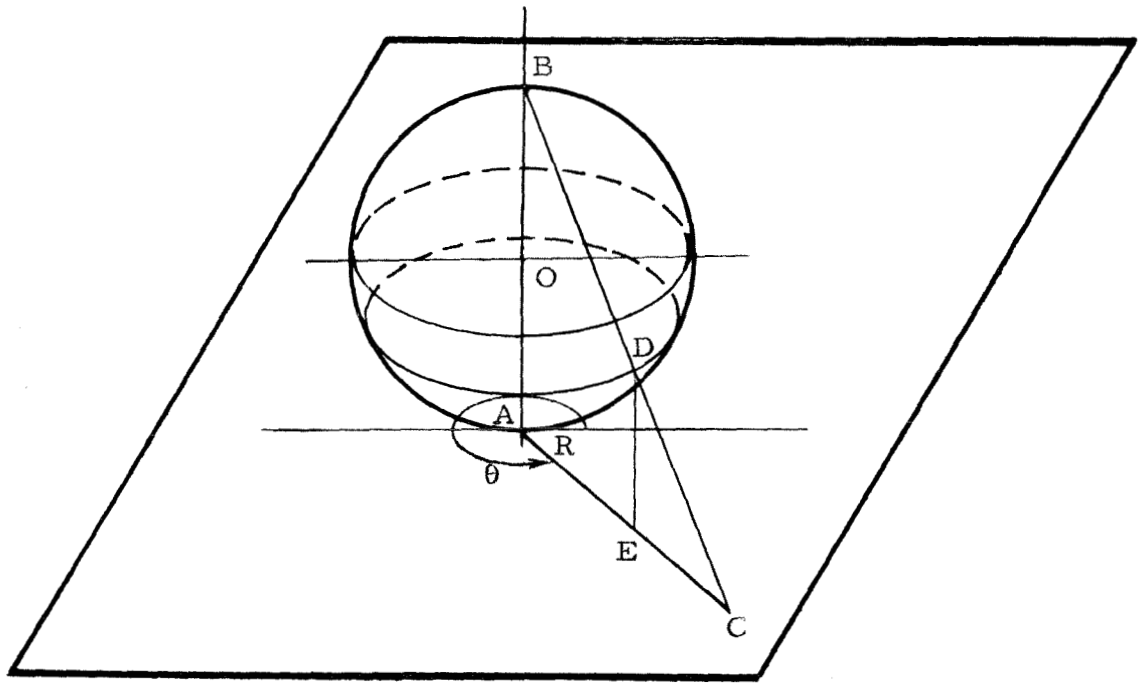

FIGURE 4a

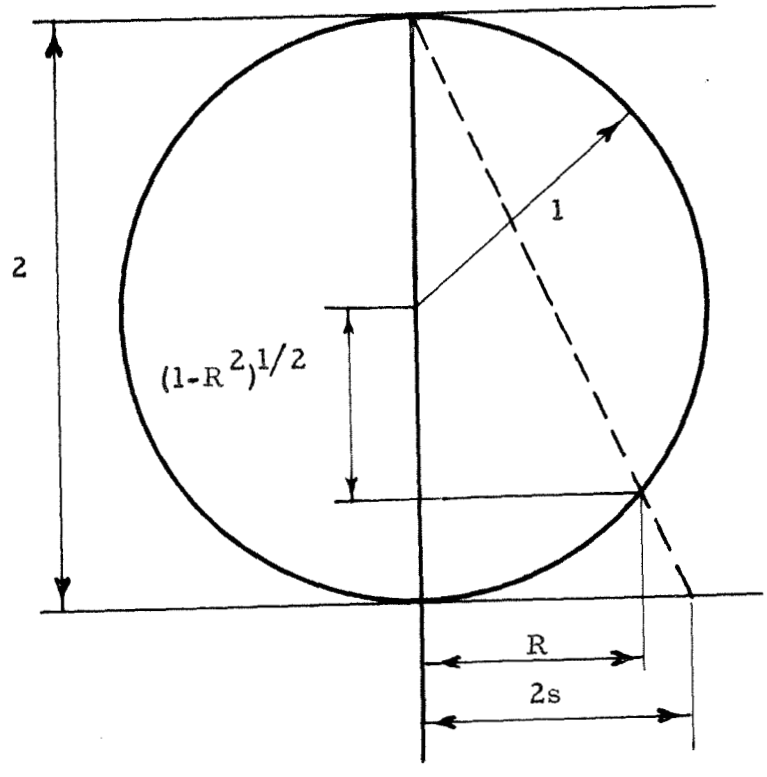

FIGURE 4b

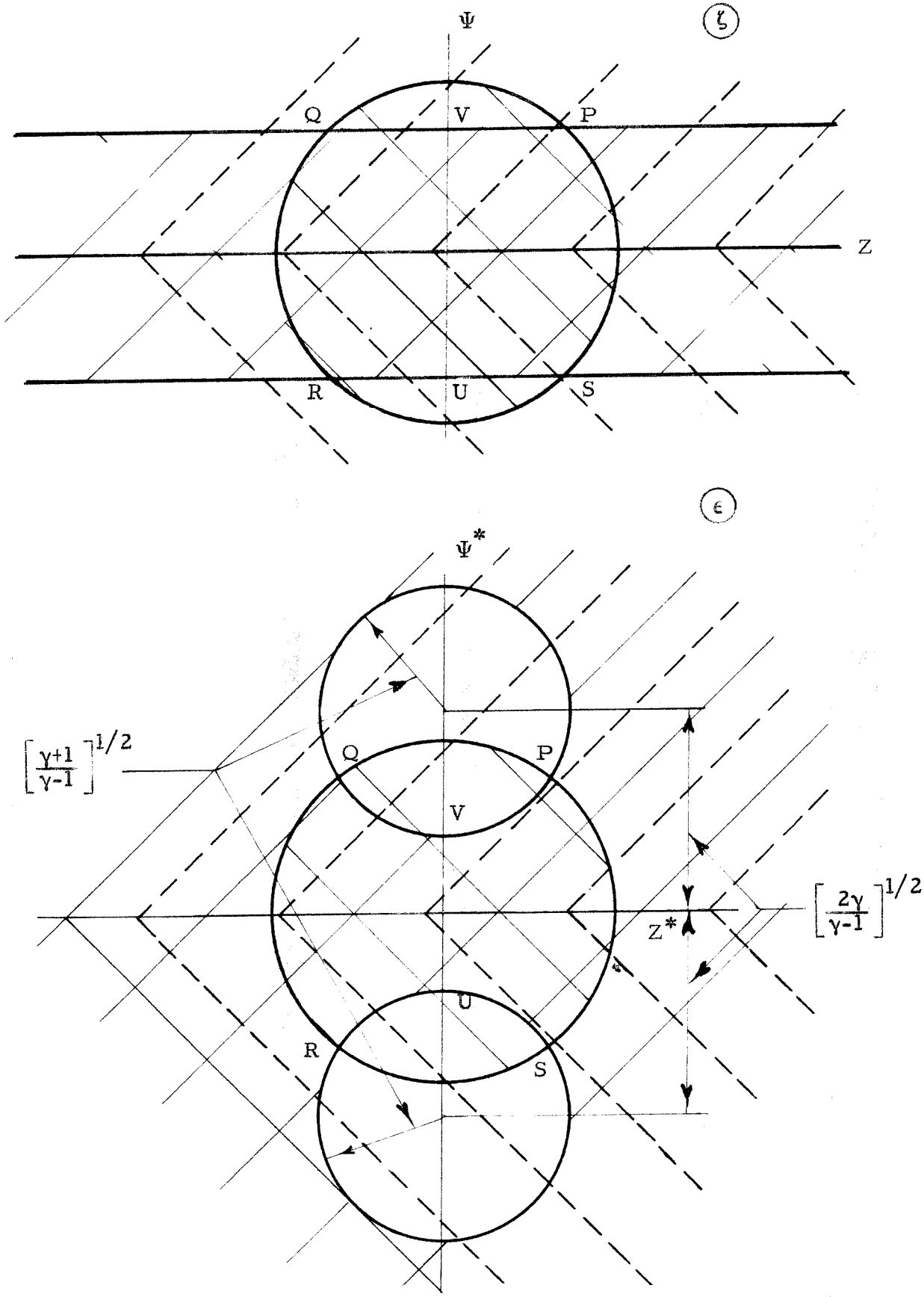

FIGURE 5

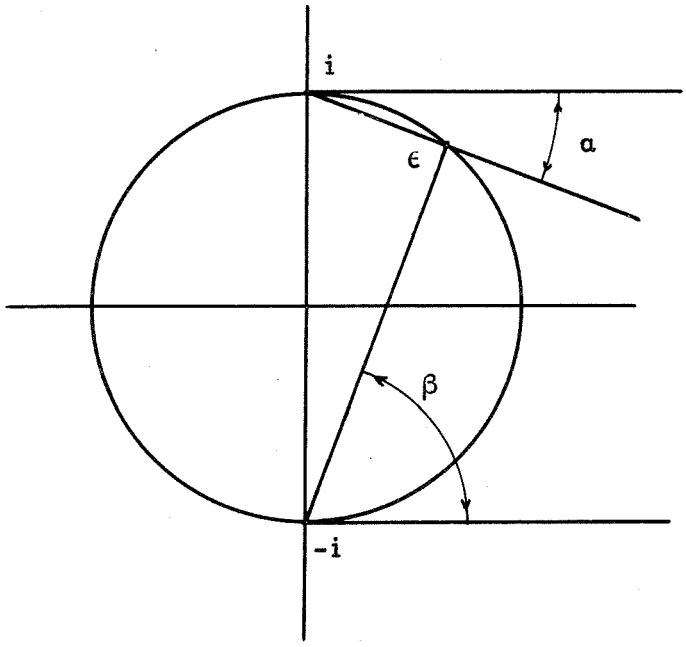

FIGURE 6a

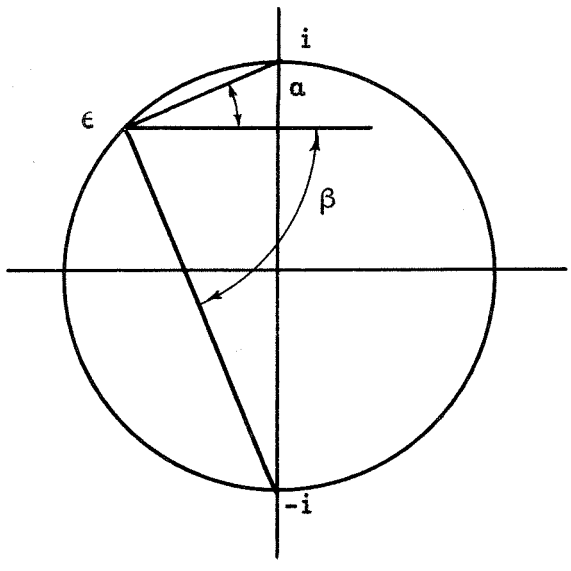

FIGURE 6b

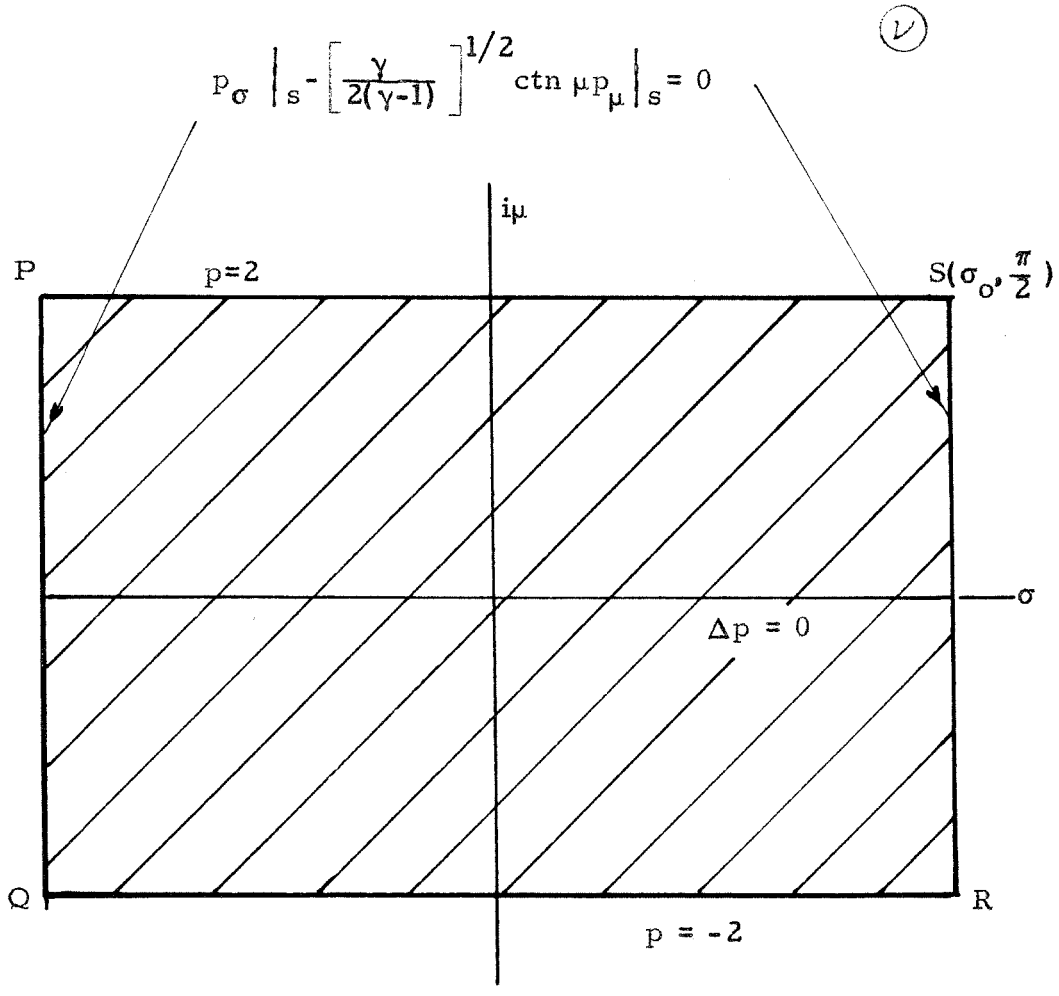
$p_\sigma\big|_s - \left[\frac{\gamma}{2(\gamma-1)}\right]^{1/2} \operatorname{ctn} \mu p_\mu\big|_s = 0$
(ν)
iμ
P
p=2
S(σ₀, π/2)
σ
Δp = 0
Q
R
p = -2

FIGURE 7

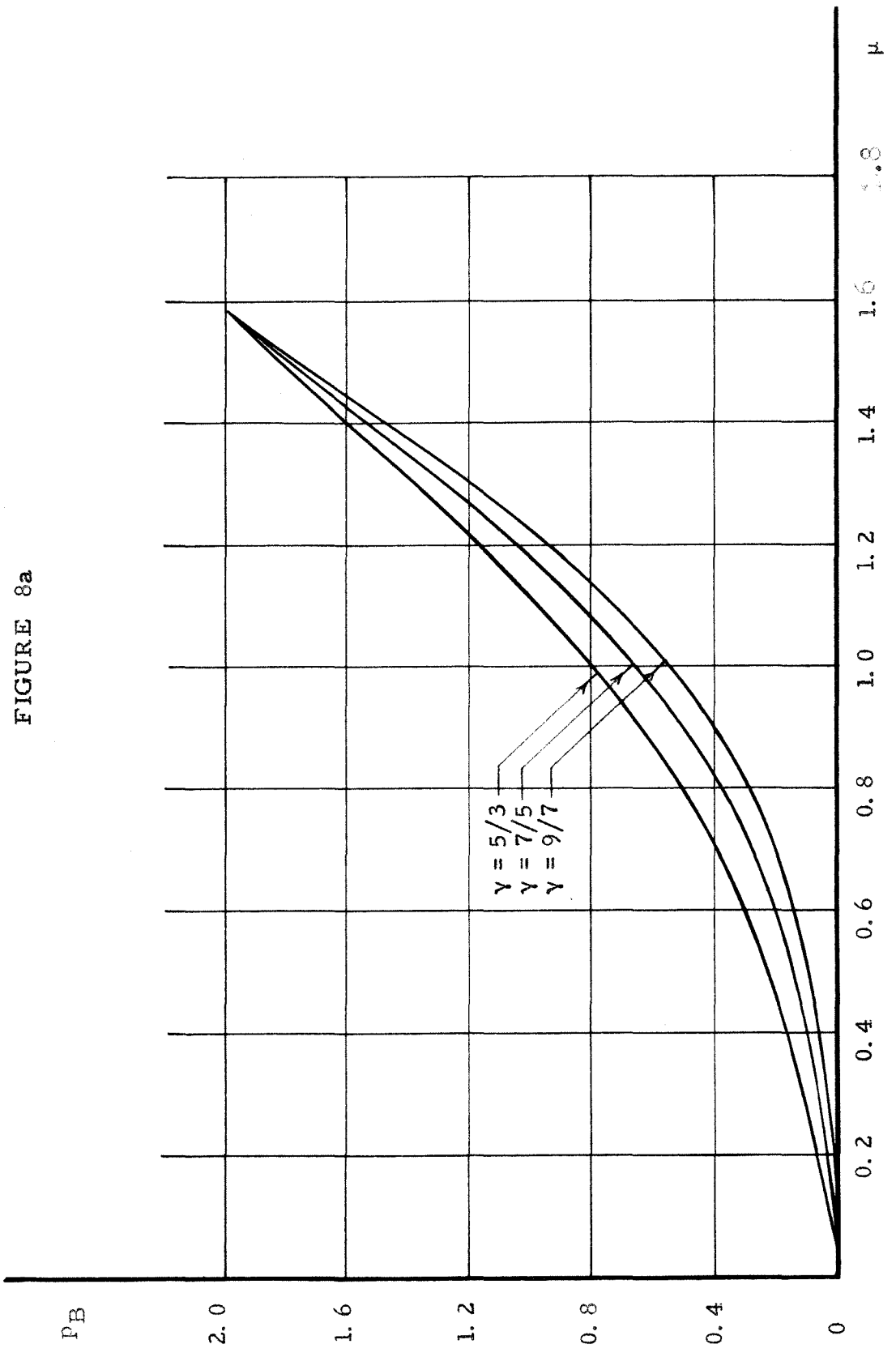

FIGURE 8a

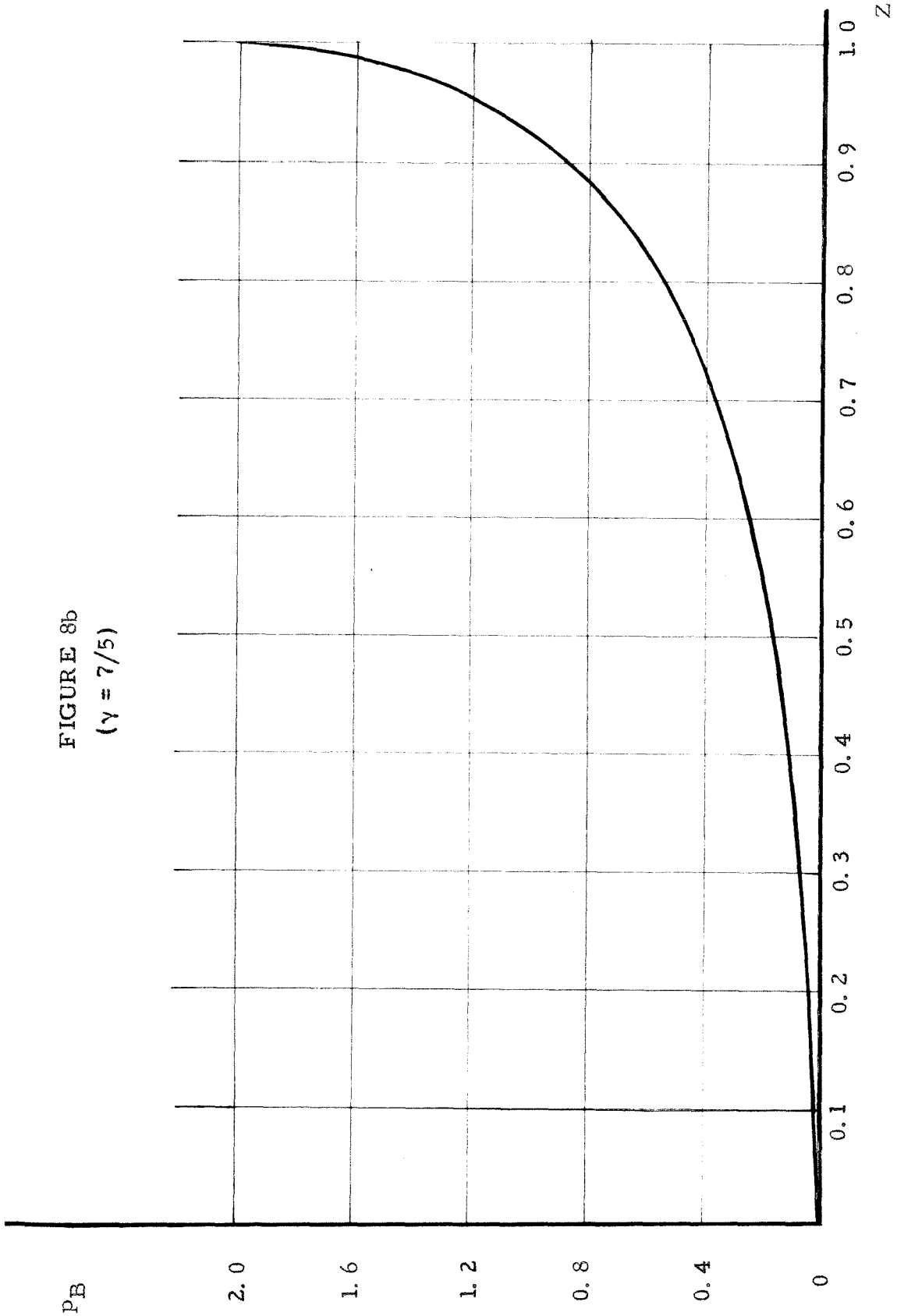

FIGURE 8b
($\gamma = 7/5$)

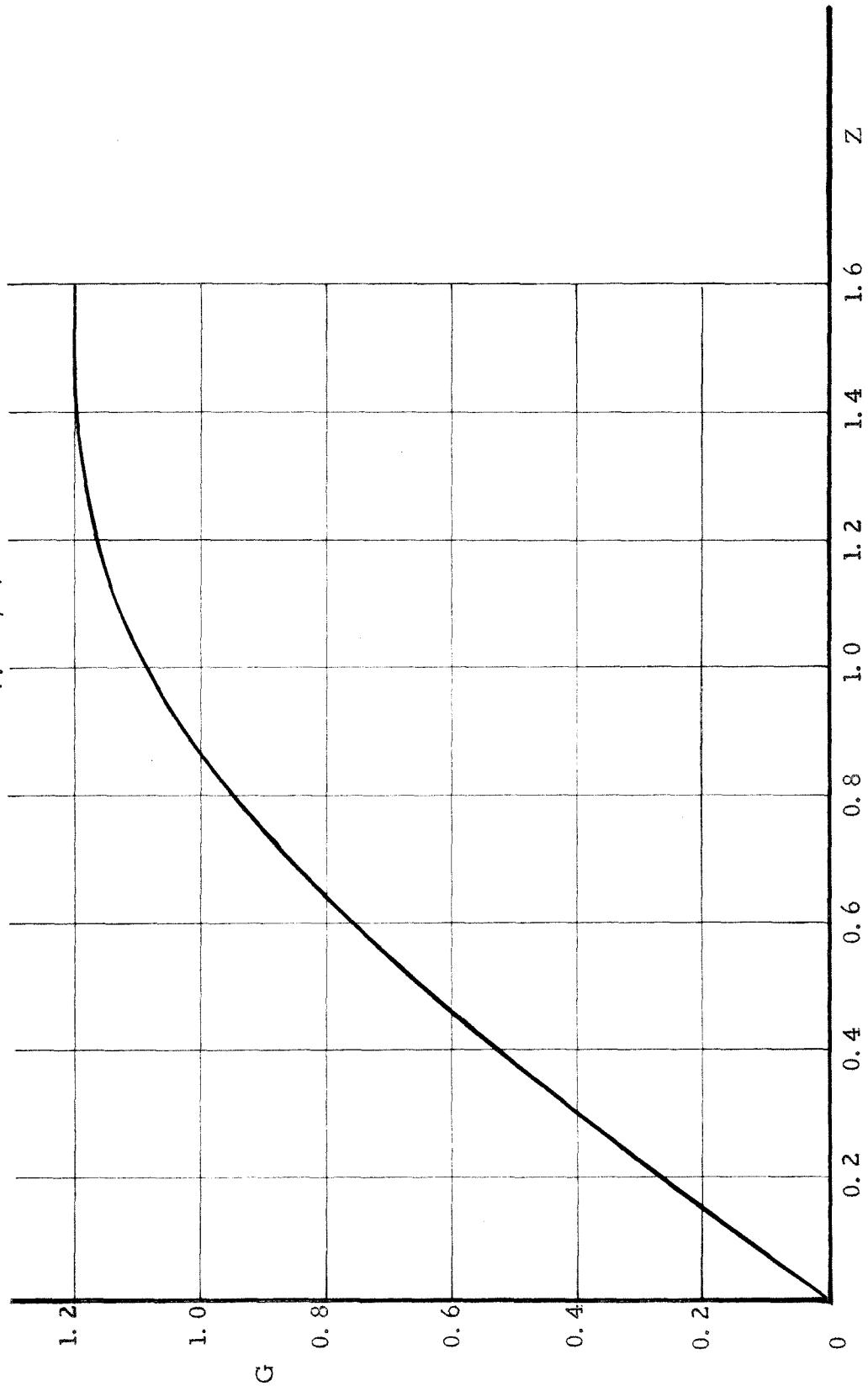

FIGURE 8c
($\gamma = 7/5$)

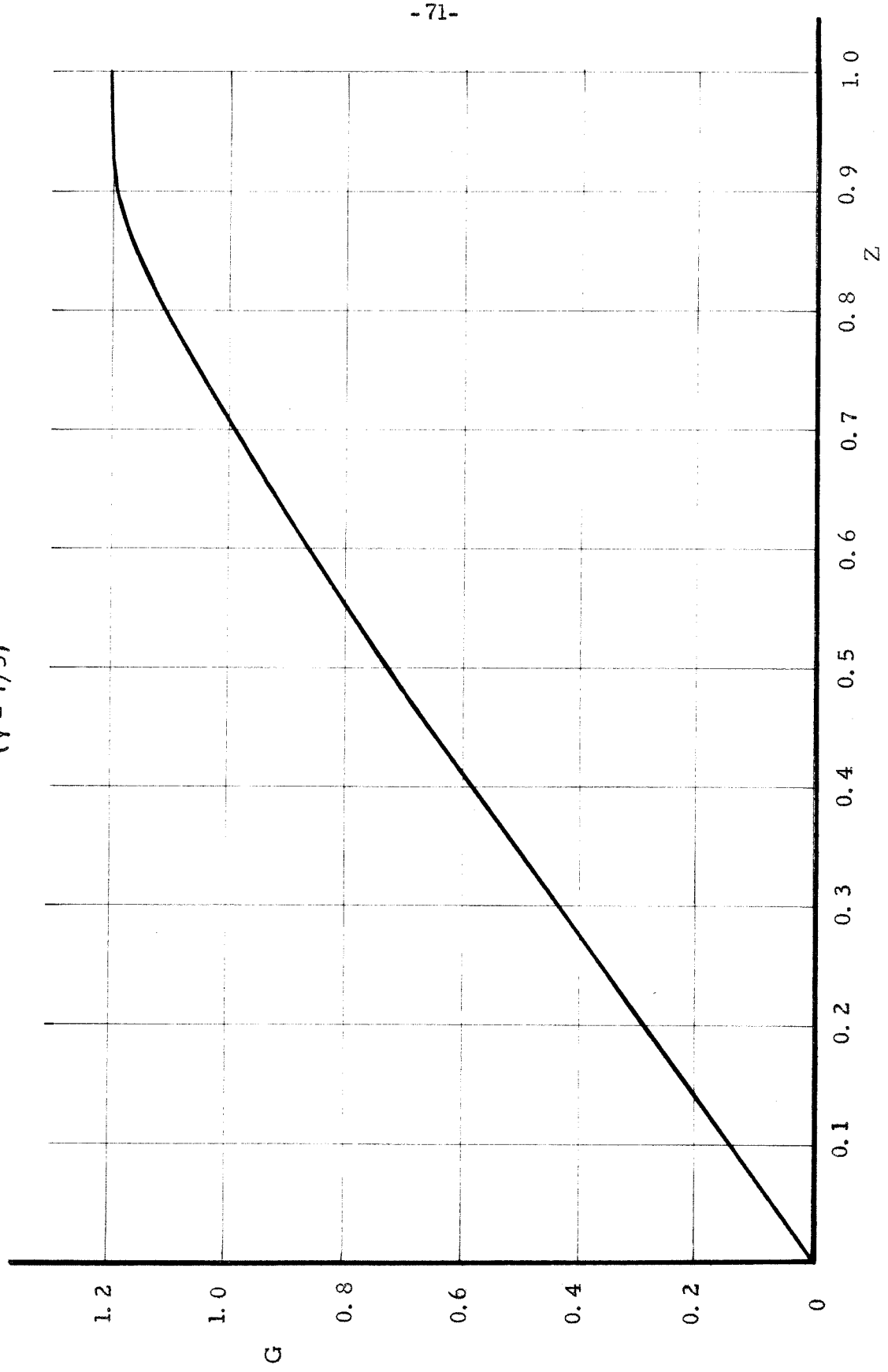

FIGURE 8d
($\gamma = 7/5$)

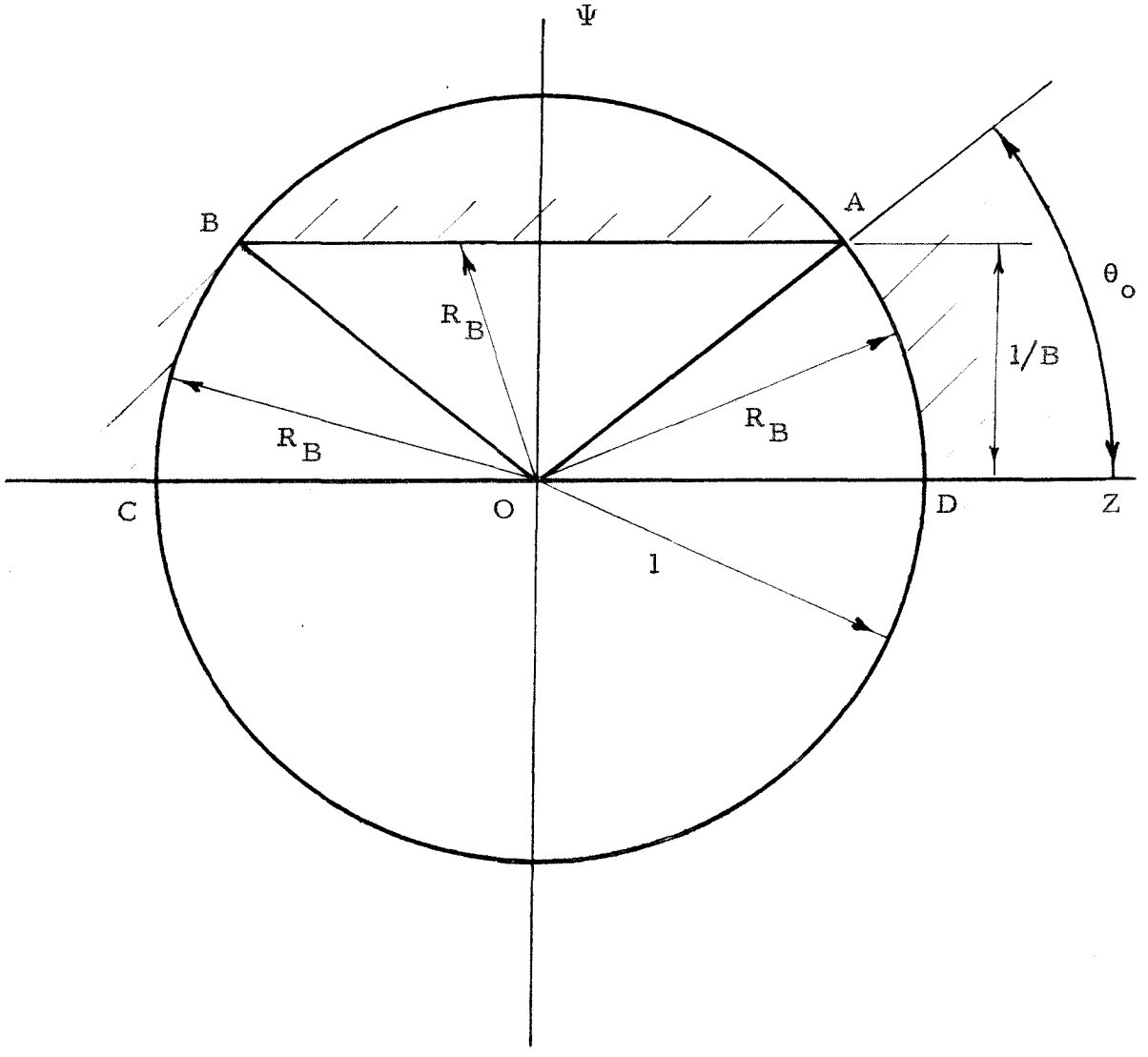

FIGURE 9

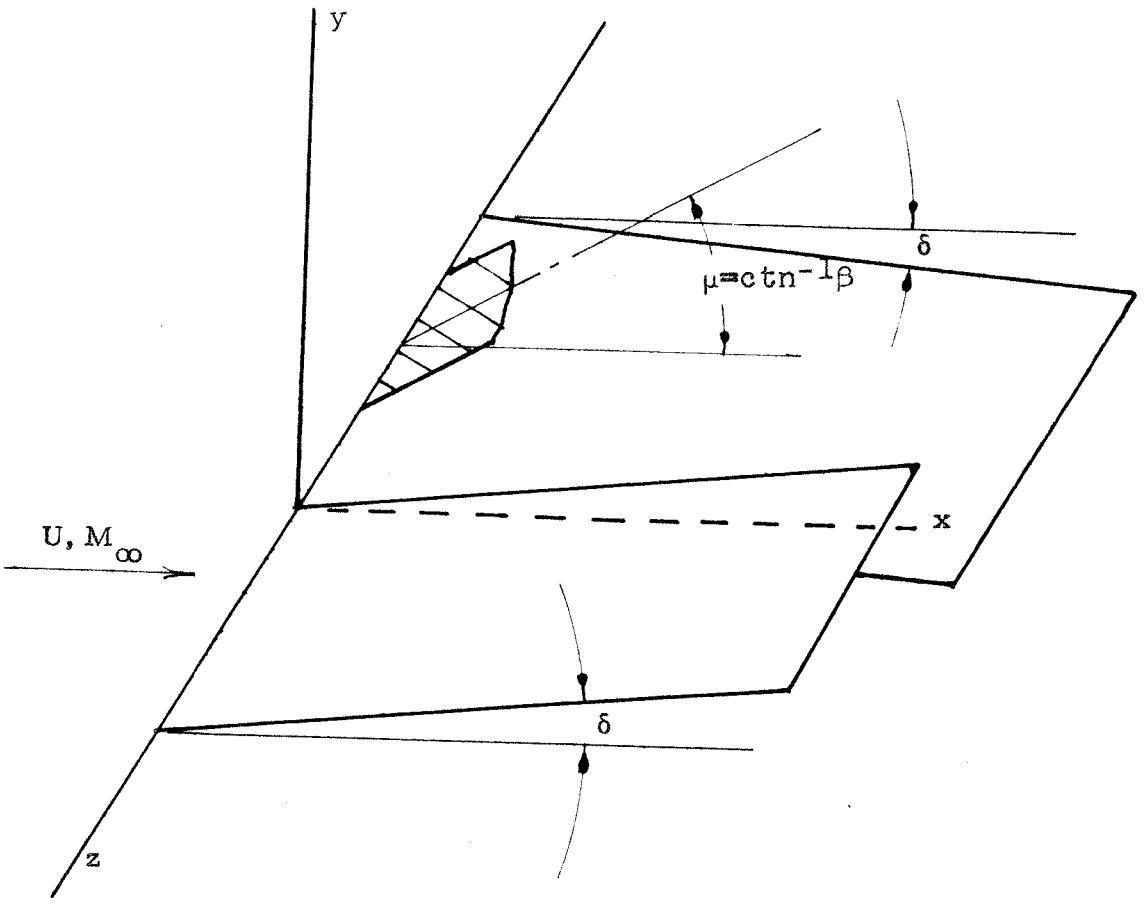

FIGURE 10

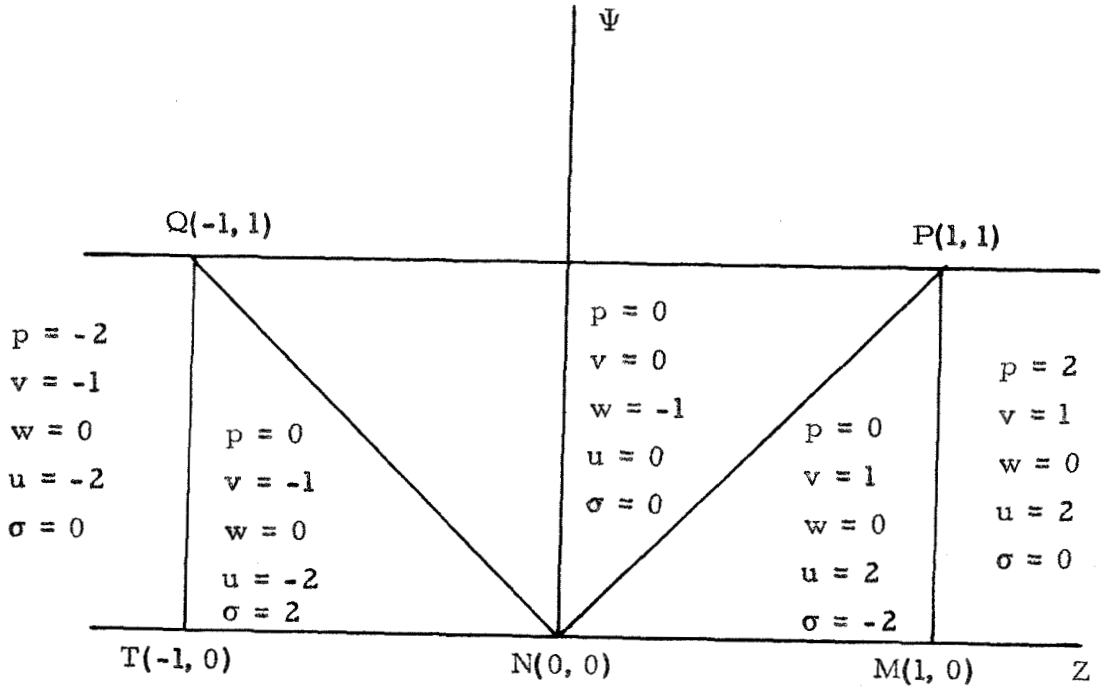
Ψ
Q(-1, 1)
P(1, 1)
p = -2
v = -1
w = 0
u = -2
σ = 0
p = 0
v = -1
w = 0
u = -2
σ = 2
p = 0
v = 0
w = -1
u = 0
σ = 0
p = 0
v = 1
w = 0
u = 2
σ = -2
p = 2
v = 1
w = 0
u = 2
σ = 0
T(-1, 0)
N(0, 0)
M(1, 0)
Z

FIGURE 11

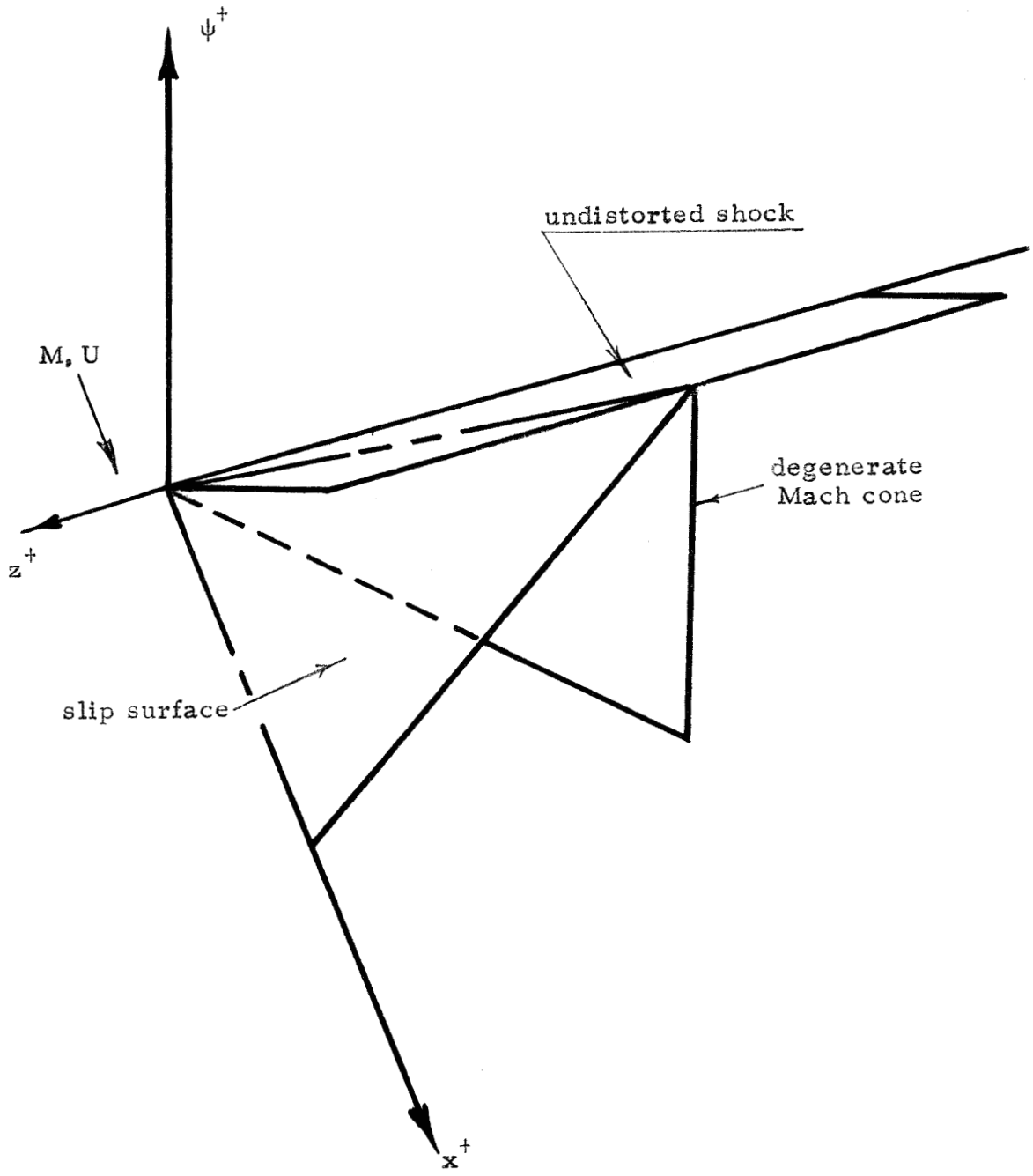
ψ+
undistorted shock
M, U
degenerate
Mach cone
z+
slip surface
x+

FIGURE 12